ARMY RESEARCH LABORATORY

Accuracy and Jump Measurements of the 5.56-mm M855 Cartridge

by Ilmars Celmins

ARL-TR-5540 **May 2011**

NOTICES

Disclaimers

The findings in this report are not to be construed as an official Department of the Army position unless so designated by other authorized documents.

Citation of manufacturer's or trade names does not constitute an official endorsement or approval of the use thereof.

Destroy this report when it is no longer needed. Do not return it to the originator.

Army Research Laboratory
Aberdeen Proving Ground, MD 21005-5066

ARL-TR-5540 **May 2011**

Accuracy and Jump Measurements of the 5.56-mm M855 Cartridge

Ilmars Celmins
Weapons and Materials Research Directorate, ARL

REPORT DOCUMENTATION PAGE	Form Approved OMB No. 0704-0188

1. REPORT DATE *(DD-MM-YYYY)*	2. REPORT TYPE	3. DATES COVERED (From - To)
May 2011	Final	April 2006–April 2007

4. TITLE AND SUBTITLE
Accuracy and Jump Measurements of the 5.56-mm M855 Cartridge

5a. CONTRACT NUMBER

5b. GRANT NUMBER

5c. PROGRAM ELEMENT NUMBER

6. AUTHOR(S)
Ilmars Celmins

5d. PROJECT NUMBER
AH80

5e. TASK NUMBER

5f. WORK UNIT NUMBER

7. PERFORMING ORGANIZATION NAME(S) AND ADDRESS(ES)
U.S. Army Research Laboratory
ATTN: RDRL-WML-E
Aberdeen Proving Ground, MD 21005-5066

8. PERFORMING ORGANIZATION REPORT NUMBER
ARL-TR-5540

9. SPONSORING/MONITORING AGENCY NAME(S) AND ADDRESS(ES)

10. SPONSOR/MONITOR'S ACRONYM(S)
PM-CAS

11. SPONSOR/MONITOR'S REPORT NUMBER(S)

12. DISTRIBUTION/AVAILABILITY STATEMENT
Approved for public release; distribution is unlimited.

13. SUPPLEMENTARY NOTES

14. ABSTRACT
The U.S. Army Research Laboratory (ARL) performed a jump test and analysis to evaluate the accuracy of the M855 projectile when fired from the M4 weapon system, and from a Mann barrel for comparison. The firings consisted of a four 10-round groups, each in a different configuration, fired through the ARL Aerodynamics Experimental Facility spark range. The performance from two different standard barrels was similar. Removal of the compensator resulted in slightly increased muzzle motion, which can be attributed to removal of mass from the muzzle. The Mann barrel exhibited drastically reduced muzzle motion. The largest jump component dispersion contributors for all four configurations were the relative center of gravity (CG) jump and the aerodynamic jump. Strong interactions were identified between relative CG jump and aerodynamic jump, which served to reduce the total jump. The overall effect of the compensator was positive, in that it resulted in lower total jump dispersion due to strengthened negative correlations. For the Mann barrel, there was a decrease in magnitude and dispersion of all jump components, most likely due to the fact that lower gun motion imparted smaller linear and angular impulses to the bullet. One implication is that the Mann barrel provides a significantly different dynamic launch environment than the standard M4 weapon, which must be taken into consideration when using Mann barrels to evaluate ammunition performance other than aerodynamics.

15. SUBJECT TERMS
accuracy, jump, small-caliber, M855, M4

16. SECURITY CLASSIFICATION OF:			17. LIMITATION OF ABSTRACT	18. NUMBER OF PAGES	19a. NAME OF RESPONSIBLE PERSON
a. REPORT	b. ABSTRACT	c. THIS PAGE			Ilmars Celmins
Unclassified	Unclassified	Unclassified	UU	48	19b. TELEPHONE NUMBER (*Include area code*) (410) 306-0781

Contents

List of Figures

List of Tables

Acknowledgments

The author gratefully acknowledges contributions from the following U.S. Army Research Laboratory (ARL) personnel:

- The ARL Aerodynamics Experimental Facility technicians: Mr. Tom Puckett who acted as test director, explosives operator, and gunner; Mr. Donald McClellan for setup, film, and experience; and Mr. Kenneth Paxton for setup, film, and data acquisition.
- Mr. Robert Kepinger for measuring and recording projectile physical parameters.
- Joyce Smith, Ronald Anderson, and Gregory Watt for reading the spark range film.
- Dr. Sidra Silton for assistance with the data reduction of the range measurements, and for technical review of this report.
- Mr. Bernard Guidos for technical guidance with data reduction and analysis.

INTENTIONALLY LEFT BLANK.

1. Introduction

The U.S. Army Research Laboratory (ARL) is participating in a program to improve the effectiveness of U.S. Army small arms weapon systems. As part of this program, an analysis of the accuracy of small arms weapon systems is being conducted. A commonly used tool for evaluating the accuracy of gun systems is the jump test, as described in reports by Celmins (*1*) and Bornstein et al. (*2*). Jump component characterization defines aspects of weapon system accuracy not directly attributable to launch velocity variability or human aiming error.

Quantification of the contributions to total accuracy of this system provides an understanding of the largest and smallest sources of error (i.e., dispersion). Such an understanding is valuable for assessing potential and actual design modifications.

This report documents jump testing and analysis performed by ARL to evaluate the accuracy of the M855 projectile when fired from the M4 weapon system, and from a Mann barrel for comparison. The data collected consists of four 10-round groups fired through the ARL Aerodynamics Experimental Facility (AEF) spark range located at Aberdeen Proving Ground, MD. From this data the jump components can be quantified allowing identification of the largest and smallest contributions to dispersion. Additionally, correlations between jump components are investigated and the effect of the muzzle compensator on accuracy is evaluated. Finally, the M4 performance is compared with that of a Mann barrel in an attempt to isolate gun dynamic effects on accuracy.

2. Jump Testing Overview

2.1 Jump Component Description

Jump testing is the methodology that measures the individual components that contribute to the projectile jump (the angular deviation between the aim point and impact point). For these tests, the jump was separated into five basic components, briefly described in the following bullet points. For a more detailed description, see Celmins (*1*) and Bornstein et al. (*2*).

- Static Pointing Angle: The angle between the gun muzzle and the line of fire (LOF) just before the trigger is pulled. This accounts for muzzle motion between the time the gun is boresighted and the shot is fired. Motion could be due to the weight of the borescope, bumping the barrel when removing the borescope, and barrel motion due to loading the cartridge.
- Muzzle pointing angle: The angle between the gun muzzle at the instant of shot exit and the pre-shot LOF when the trigger is pulled.

- Muzzle crossing velocity: The angular deflection of the trajectory produced by the gun muzzle transverse velocity. This angle is computed from the arctangent of the ratio of the gun muzzle transverse velocity at the instant of shot exit to the projectile exit velocity.
- Center of gravity (CG) jump: The angle of the projectile CG initial trajectory. The *absolute* CG jump is the angle of the initial trajectory relative to the pre-shot LOF. The *relative* CG jump is the angle of the initial trajectory relative to a muzzle-attached coordinate system. In the current measurement methodology, the relative CG jump is calculated by subtracting the sum of the muzzle pointing angle and muzzle crossing velocity jump components from the absolute CG jump.
- Aerodynamic jump: The angle between the projectile's downrange trajectory and the initial trajectory angle. Aerodynamic jump is the result of the integrated effect of aerodynamic lift due to the yawing motion of the projectile. Aerodynamic jump is calculated using the initial angles and angular rates of the projectile.

The jump components are vector quantities, measured in a coordinate system whose origin is the pre-shot LOF. The jump components are usually measured in milliradians (mrad).

The CG jump and aerodynamic jump components are calculated using quantities determined as the projectile enters free flight. This location is chosen to be a few calibers from the muzzle, as the projectile emerges from the muzzle blast. Strictly speaking, the CG jump and aerodynamic jump contain lateral and angular disturbances imparted by asymmetry that may exist in the muzzle blast.

The total jump for a given shot can be calculated by adding together the individual jump components. The total jump can then be compared to the hole in the target, and the difference between the two is referred to as the "closure error."

2.2 Jump Component Measurements

The testing was performed at the ARL AEF (*3*). Various types of instrumentation and measurement techniques were used to measure the jump components described in the previous section. A brief overview of the measurement techniques follows.

2.2.1 Line of Fire

The LOF is a line connecting the center of the muzzle with the aimpoint on the target, where the aimpoint is defined as the location on the target to which the muzzle points, i.e., the boresight point. The LOF defines the origin for the jump vectors—all the jump angles are measured relative to the angle of the LOF.

In order to get the LOF in range coordinates, both the muzzle location and aimpoint were specified in range coordinates as follows. First, the gun was boresighted (figure 1) in the approximate center of the range. Next, a cable with a set of crimped, light weight beads (fiducial

cable) was hung passing through the gun muzzle and also through the first group of range stations (figure 2). This cable was then photographed in the range, and the data was processed to get the locations of the beads in range coordinates. The range cable measurements were then extrapolated back to get the muzzle location in range coordinates. The cable was then removed and a target was placed within the field of view of the last range station (station 300, nominally 88.2 m from the muzzle). The aimpoint of the boresight was marked on the target and a pushpin was inserted at the aimpoint (figure 3). This pushpin could be seen on the range film so its location could be determined in range coordinates. The extrapolated muzzle location and the measured aimpoint were then used to calculate the LOF in range coordinates.

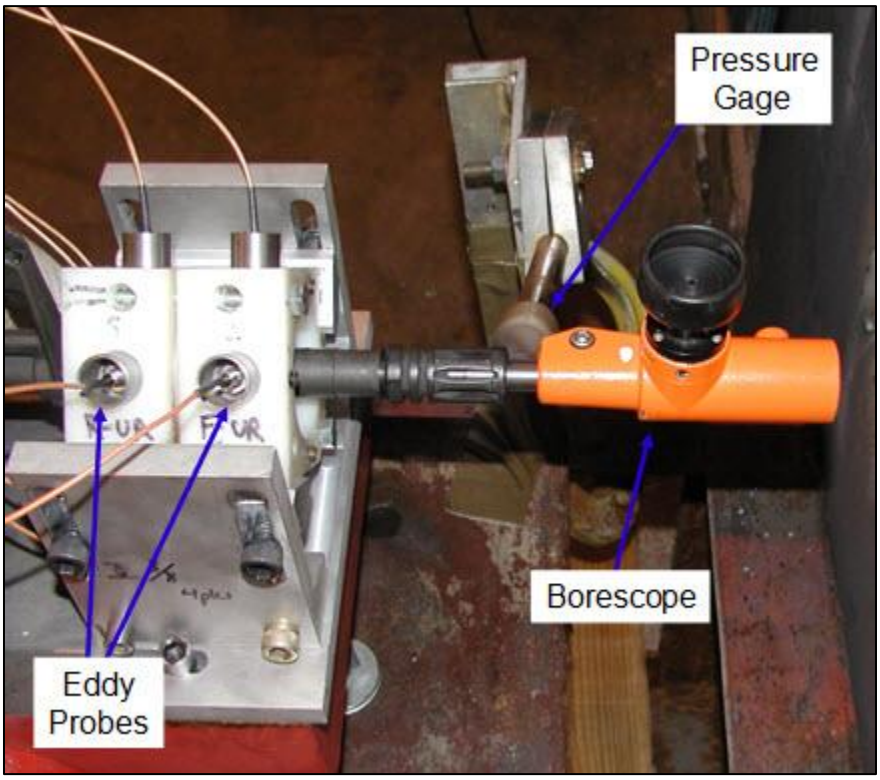

Figure 1. Gun muzzle, borescope, eddy probes, and pressure gage (for triggering instrumentation).

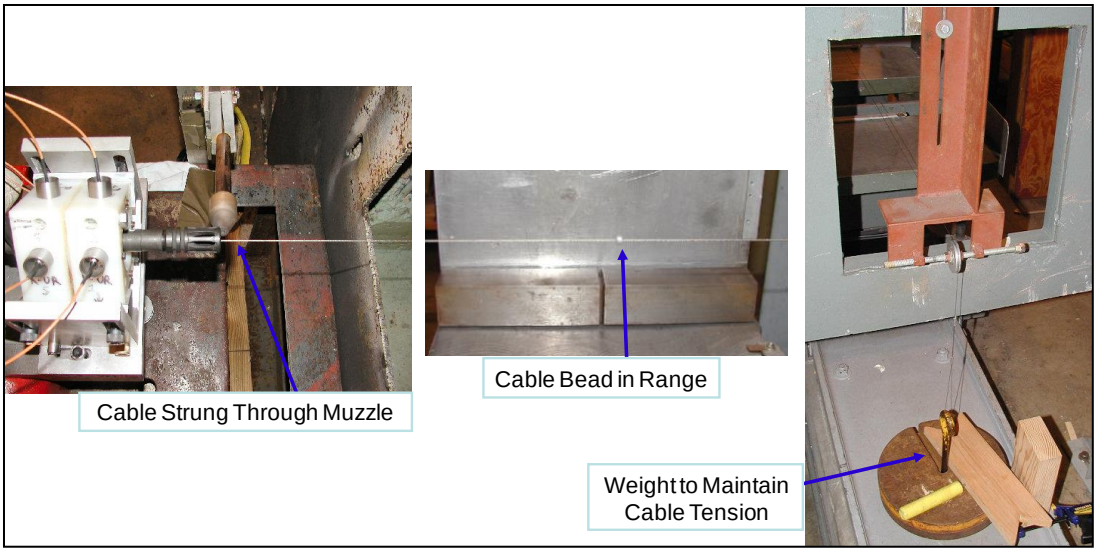

Figure 2. Fiducial cable.

Figure 3. Target with pushpin in place.

2.2.2 Gun Tube Motion

The motion of the gun tube was measured using inductive proximity probes (eddy probes) located near the muzzle. The eddy probes, when coupled with the appropriate drivers, generate an output voltage that is proportional to the gap between the probe and a conducting surface.

When multiple probes are arranged along the circumference of a gun tube, the individual gap measurements can be combined to calculate the location of the center of the gun tube, as discussed in reports by Celmins (*1*) and Bornstein et al. (*2*, *4*).

Using two sets of eddy probes offset along the gun axis results in two bore centerline measurements. The difference between these measurements can be used to calculate the instantaneous muzzle pointing angle. An extrapolation from the two measurements to the muzzle yields the muzzle position. The time rate of change in muzzle position is the muzzle crossing velocity. The muzzle motion measurements are taken using a common time base with the shadowgraph trajectory measurements. This common time base allows shot exit time to be calculated and the muzzle conditions at the time of shot exit to be determined. The common base time is obtained using a pressure gage to trigger the range instrumentation at shot exit (figure 1).

2.2.3 Projectile Motion

The projectile downrange motion could be measured directly because the jump tests were conducted at the AEF spark range (figure 4). This facility has 39 direct-image orthogonal spark shadowgraph stations, divided into five groups spread over a distance of ~100 m. As a projectile flies through the range, orthogonal shadowgraphs are taken at each station. The shadowgraph images are then measured to obtain the projectile's position and angular orientation along its flight path.

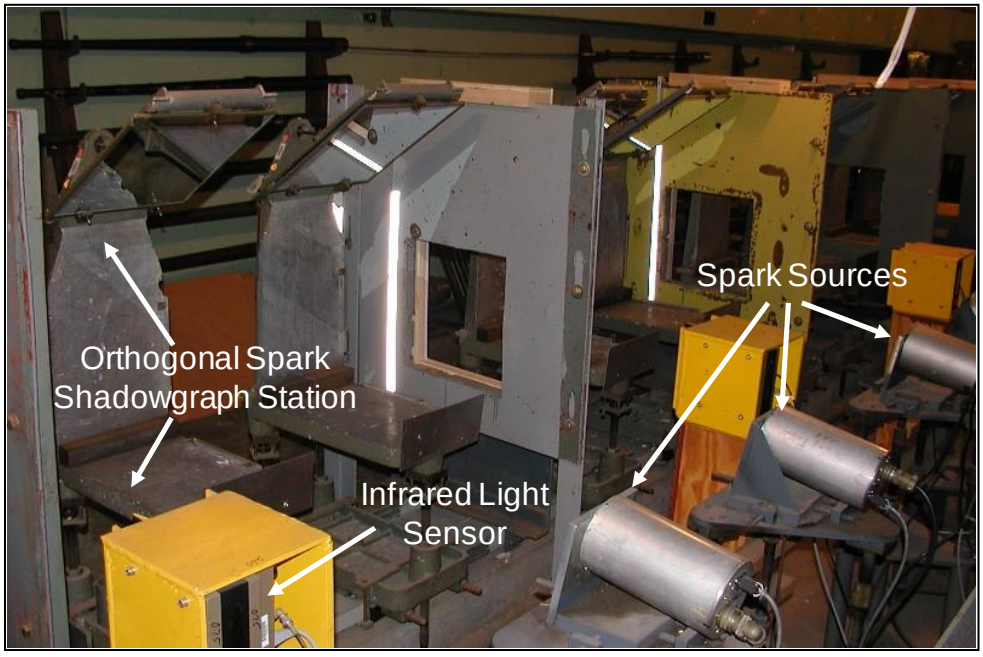

Figure 4. View of ARL AEF indoor spark range.

Figure 5 shows the shadowgraph film for shot 26951, station 75V, and figure 6 shows a magnified positive image of the same piece of film. The film designation represents the downrange distance from the range origin (located near the gun position) in feet and the film orientation (H indicates horizontal motion and V indicates vertical motion). The focused image is the projectile shadow exposed directly onto the film. The projectile shadow, rather than the projectile itself, is used to construct discrete angular and positional data. The bottom edge of the film and the triangular marker are surveyed reference indicators. The developed film is produced as a negative image. Each piece of negative image film is manually read on a precision light table to produce the measured spatial coordinates (range, deflection, altitude) and angular orientation (pitch, yaw, roll) relative to an earth fixed-range coordinate system, all as a function of the spark time. The discrete values are used to construct 6-degree-of-freedom (6-DOF) models of projectile motion that allow characterization of the aerodynamics and flight dynamics.

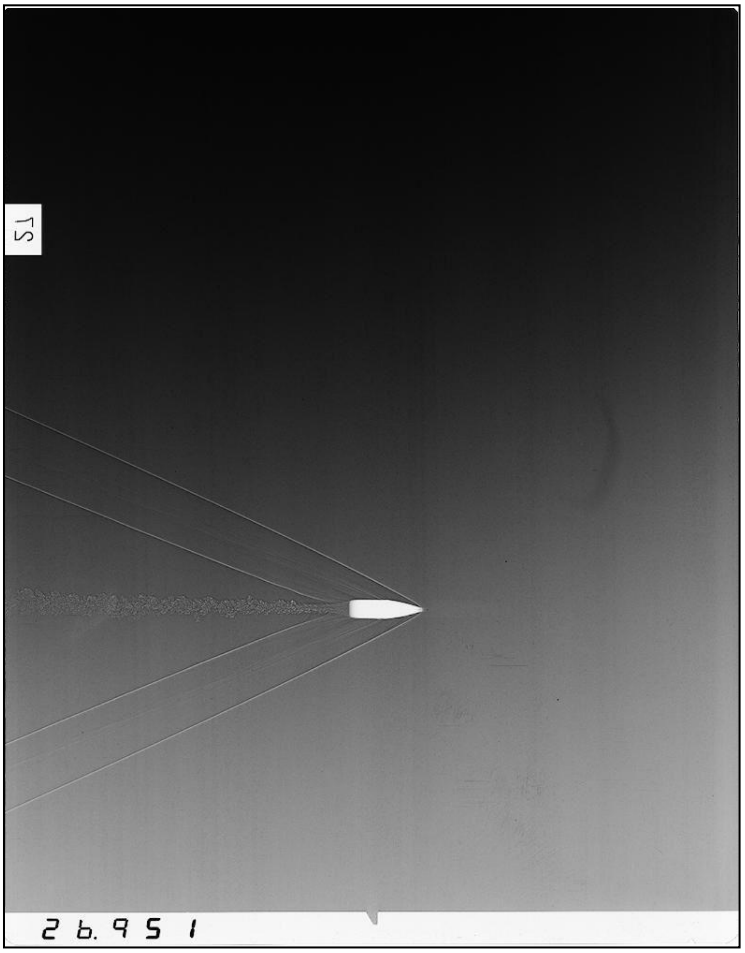

Figure 5. Shadowgraph, M855, shot 26951, station 75V.

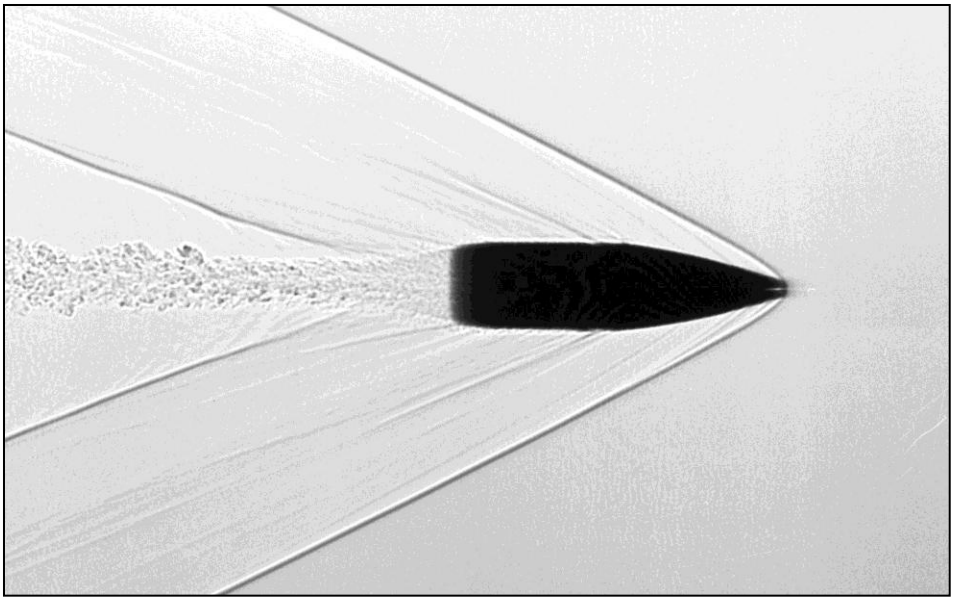

Figure 6. Shadowgraph positive image, M855, shot 26951, station 75V.

After the film was read, the data was reduced using ARFDAS (*5*). The resulting 6-DOF fit to the data provided the projectile position and angular orientation at any point along its flight. This fit was extrapolated back to the muzzle to get the conditions (CG trajectory, angles, and angular rates) when the projectile first entered free flight, i.e., initial conditions. The initial conditions were then used to calculate the CG jump and aerodynamic jump components.

2.2.4 Target Impact

The target impact point was measured directly on the paper target that was previously described for measuring the LOF and shown in figure 2. The boresighted aimpoint was marked on the target and the horizontal and vertical distance from this point to the hole made by the bullet was measured directly.

2.2.5 Gravity Drop

Gravity drop is calculated individually for each shot using the fitted 6-DOF time of flight (using $\frac{1}{2}gt^2$), as described in Celmins (*1*). For jump calculations, the gravity drop is used to adjust the measured impact point. This is done because all of the standard jump components are angular quantities that do not change with distance. If gravity drop were included as a jump component, the jump diagram and calculations would only be valid at a specific distance.

3. Projectile, Weapon, and Mount

The M855 used in this test (figure 7) is the current U.S. Army standard issue cartridge, weighing 62 gr, and has a lead alloy core with a steel insert. The projectiles belonged to reference lot LC-87F000R011.

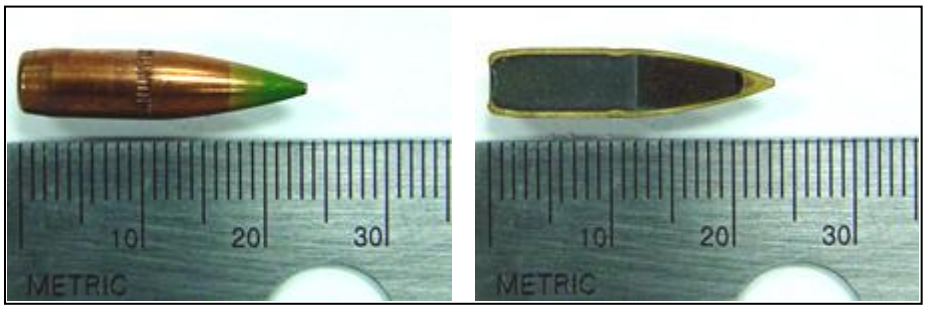

Figure 7. Intact and sectioned M855 projectile.

Table 1 lists the nominal physical properties of the M855 projectile used in this study. The physical property measurements were made by ARL on five M855 projectiles from Lot LC-87F000R011. Data analysis was performed assuming nominal physical properties for all projectiles.

Table 1. M855 projectile physical properties.

Dimension	Average Value	Std. Dev. (% of Average)
Reference diameter (mm)	5.68	0.3
Mass (g)	4.036	0.3
Length (mm)	23.06	0.4
CG from nose (mm)	14.28	1.4
Axial moment of inertia (g-cm^2)	0.1416	0.4
Transverse moment of inertia (g-cm^2)	1.1385	1.0

The firings were conducted using two different mounts, one for an M4 weapon (figure 8) and one for a Mann barrel (figure 9). Two different gun barrels were used with the M4, designated barrel no. 1 and barrel no. 2. For barrel no. 1, a single group was fired with the muzzle compensator installed. Two groups were fired from barrel no. 2: one with the muzzle compensator in place, and one with a bare muzzle. An additional group was fired from a Mann barrel, serial number KSA014, without a compensator. For each configuration, a 10-shot group was fired. To summarize, the four configurations tested were:

- M4, barrel no. 1
- M4, barrel no. 2

- M4, barrel no. 2, bare muzzle
- Mann barrel

The Mann barrel mount was a symmetric recoil mount designed to support the heavy-walled barrel as steadily as possible (figure 9).

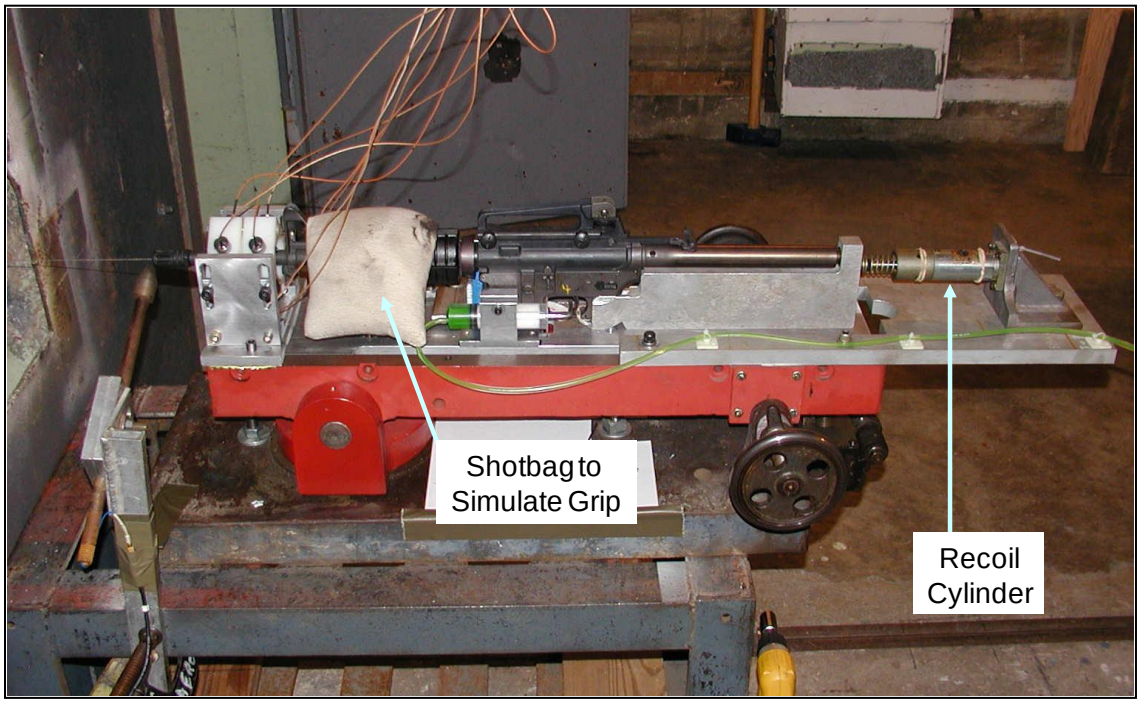

Figure 8. M4 weapon in test stand with eddy probe holder, muzzle pressure gage, and fiducial cable.

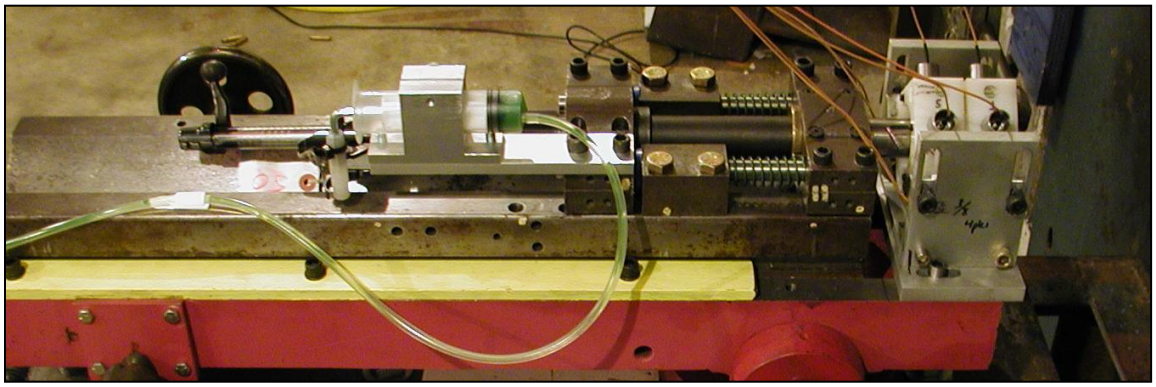

Figure 9. Mann barrel in test stand.

The design of the gun mount was crucial to the realism of the jump measurements. The M4 weapon is normally shoulder-fired. Firing the weapon off the shoulder was not a valid option for jump testing for numerous reasons. A fixed mount was needed that would replicate the shoulder-fired dynamics as much as possible, while constraining the weapon sufficiently that instrumentation was not damaged and the required measurements could be taken.

A photograph of the gun mount is shown in figure 8. The stock was removed from an M4 rifle and the rifle was attached to a vertical aluminum plate. The rifle and plate were then attached to a horizontal aluminum plate that was fitted into a Frankford Arsenal gun mount, so that it was free to slide under recoil. The recoil motion was attenuated by a spring-damper recoil cylinder. The gun handrest was supported from below and a shotbag was placed on top of the hand rest to simulate a soldier gripping the weapon. The eddy probe holder is attached to the non-moving part of the gun mount, to provide a fixed reference for the muzzle motion measurements. The total weight of the recoiling parts (with the shotbag) was 19.0 kg (41.8 lb). A hydraulic piston and cylinder was used to smoothly pull the trigger in order to avoid any added gun motion during firing.

4. Results

4.1 General Results

The temperature of the indoor facility, including the ammunition magazine within, is ~70 °F. Therefore, the projectiles, weapon, and atmospheric conditions can be considered ambient. Setup time between shots was a minimum of 30 minutes (usually 60 to 90 minutes), and as a result, the weapon experienced minimal heating.

The velocities as measured in the range corresponded to a Mach number of ~2.4. The average launch velocity was 859.4 m/s, with a standard deviation of 5.7 m/s. The lowest measured launch velocity was 849.7 m/s; the highest was 873.5 m/s.

The AEF shot numbers for the 40 shots were within the ranges of 26942–26951 and 27160–27197.

4.2 Sample Measurements and Jump Diagram for an Individual Shot

Figure 10 shows the measured gun tube lateral displacement histories at the front and rear eddy probe measurement locations. The front and rear locations were 64 and 106 mm, respectively, from the muzzle. In-bore time is estimated to be 0.95 ms. Shot exit is defined as the time at which the projectile mechanically disengages from the muzzle. The measured displacement in the vertical plane is larger than the horizontal motion at shot exit. No noticeable discontinuities in lateral tube displacement are apparent at shot exit.

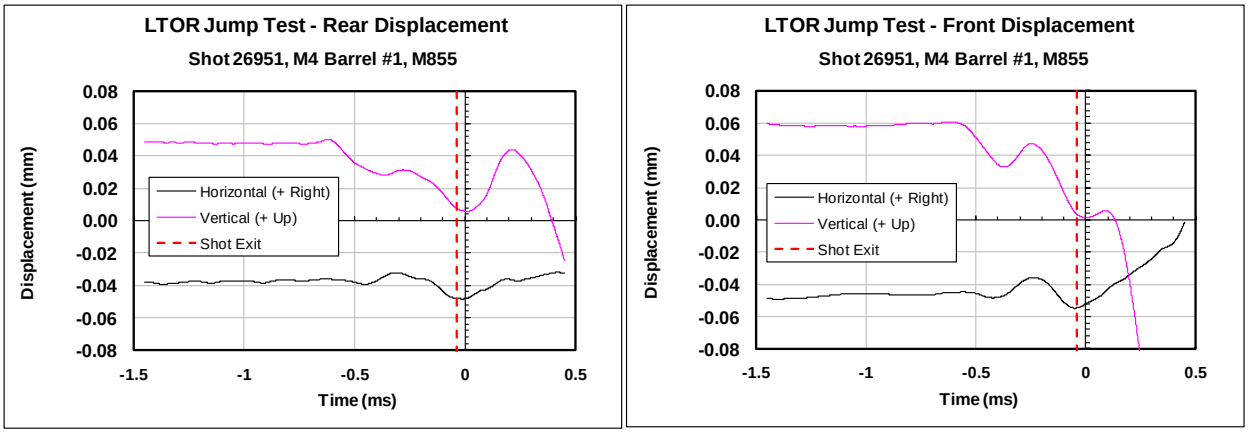

Figure 10. Launch tube lateral displacement histories, rear and front eddy probes, shot 26951.

Figure 11 shows the muzzle pointing angle history, obtained by combining the displacements measured at the front and rear probe locations. As with the displacements, the angular displacements in the vertical plane are slightly larger than those in the horizontal plane at shot exit.

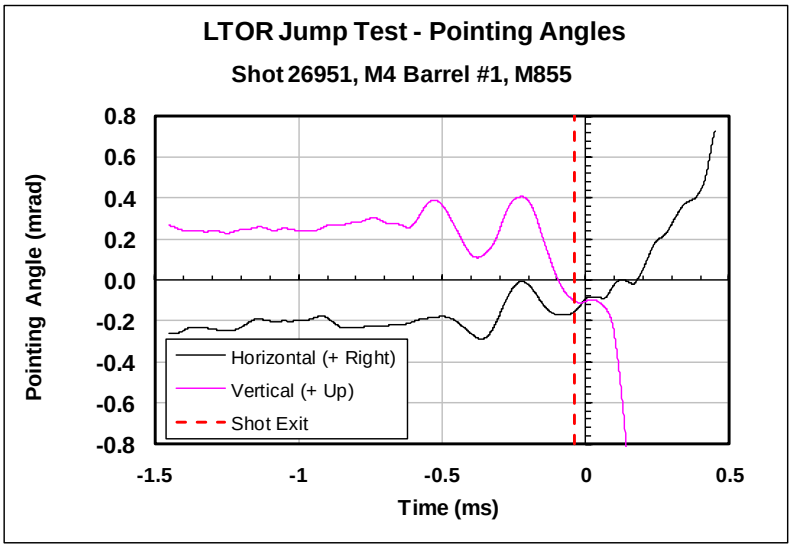

Figure 11. Muzzle pointing angle history, shot 26951.

The muzzle crossing velocity is shown in figure 12. Crossing velocity is calculated by taking the time derivative of the muzzle location, which is extrapolated from the two displacement measurements discussed previously. This calculation requires the assumption of negligible bending of the barrel from the rear gage to the muzzle. The angle computed from the arctangent of the ratio of the gun muzzle transverse velocity at the instant of shot exit to the projectile exit velocity is the crossing velocity jump component.

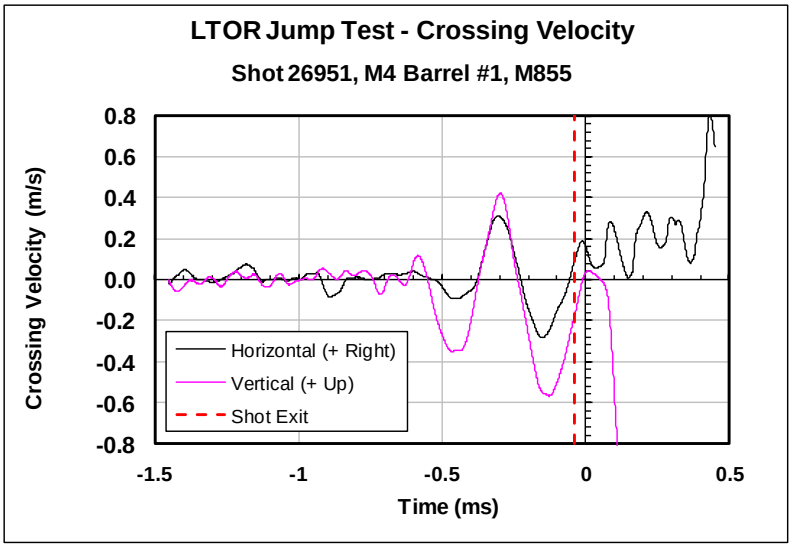

Figure 12. Muzzle crossing velocity history, shot 26951.

Figure 13 shows the horizontal and vertical CG trajectories obtained from the spark shadowgraph 6-DOF fits. Comparison is made between the CG locations measured in the range, those obtained from the 6-DOF fits, and the pre-shot LOF. The initial CG trajectory is calculated as the tangent to the extrapolated 6-DOF fit of the range data. The angle between this initial CG trajectory line and the LOF is the absolute CG jump. Within a few meters from the muzzle, the CG trajectory departs from its initial path due to the effect of aerodynamic lift and gravity drop on the projectile.

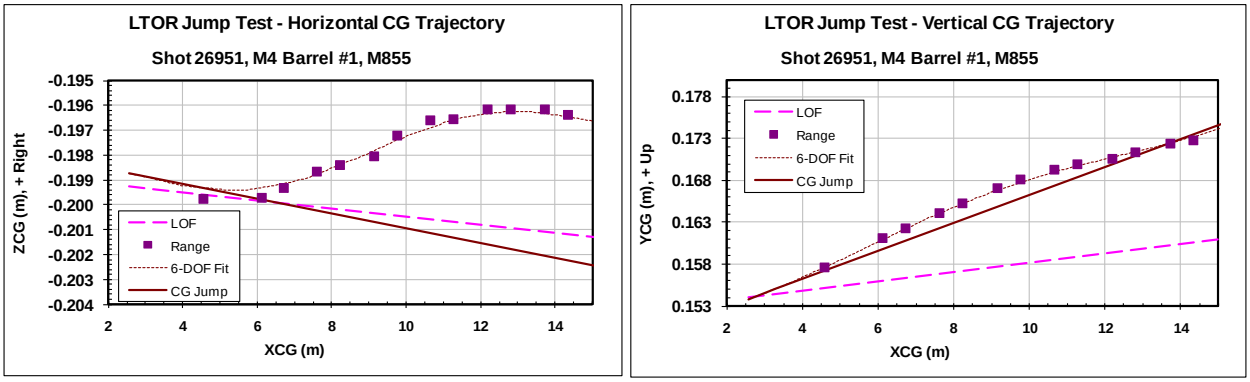

Figure 13. Horizontal and vertical CG trajectories.

Aerodynamic lift is produced because the projectile flies with pitching and yawing motion relative to its instantaneous velocity vector. Figure 14 shows the pitch and yaw angles over the trajectory for shot 26951 from the spark shadowgraphs and the 6-DOF fits. The 6-DOF fits are extrapolated uprange to determine the pitch angle, yaw angle, and their rates at shot exit. These angles and angular rates are needed to calculate the aerodynamic jump (*6, 7*) for a spin-stabilized projectile, and the procedure is outlined in Celmins (*1*).

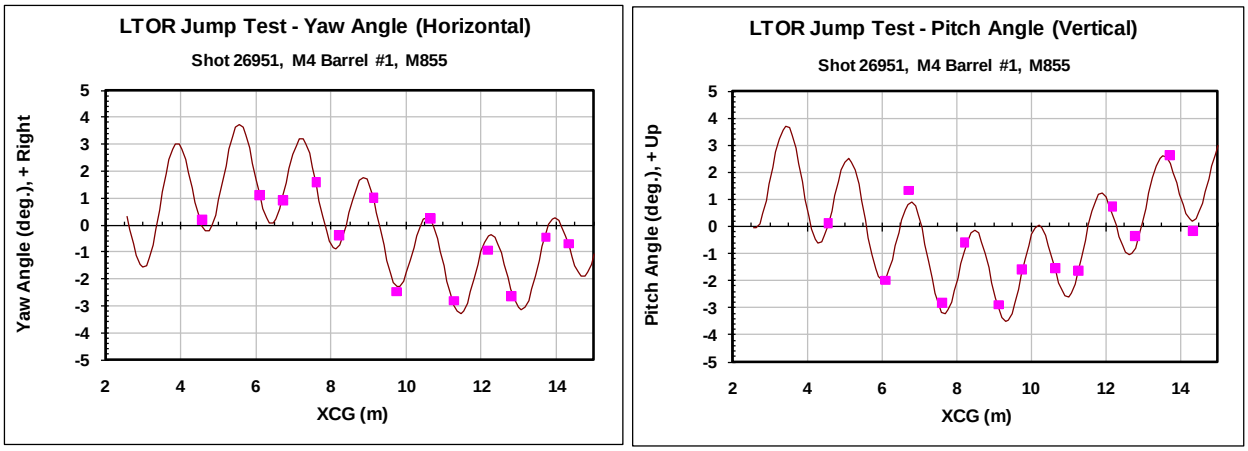

Figure 14. Projectile pitch and yaw angles through first 15 m, shot 27698.

Figure 15 shows the total angle of attack over the trajectory for shot 26951 from the spark shadowgraphs and the 6-DOF fits. The first maximum angle of attack for this shot is 3.9°, and the angular motion is damping over the displayed 15-m trajectory interval.

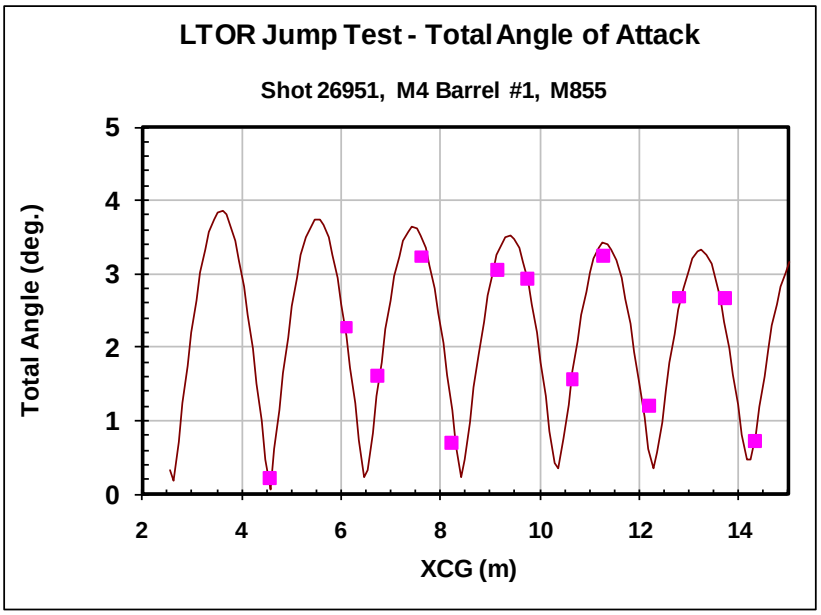

Figure 15. Projectile total angle of attack through first 15 m, shot 26951.

The jump components for a single shot can be combined into a jump diagram, as shown in figure 16. The jump diagram also includes the target impact, and a superimposed picture of the actual target showing the aimpoint and bullet hole. As described previously, the target impact is corrected for gravity drop, and figure 16 also shows the magnitude and effect of this correction. The difference between the sum of the jump vectors and the corrected impact is referred to as the closure error. For the 40 shots tested, the overall average closure error was –0.04 mrad in both the horizontal and vertical directions. Traditionally, in jump testing, good closure is declared when the magnitude of the closure error is <0.2 mrad. It should be noted that for this test setup, one bullet diameter at the target was equivalent to 0.06 mrad, so the average radial closure error was approximately one bullet diameter.

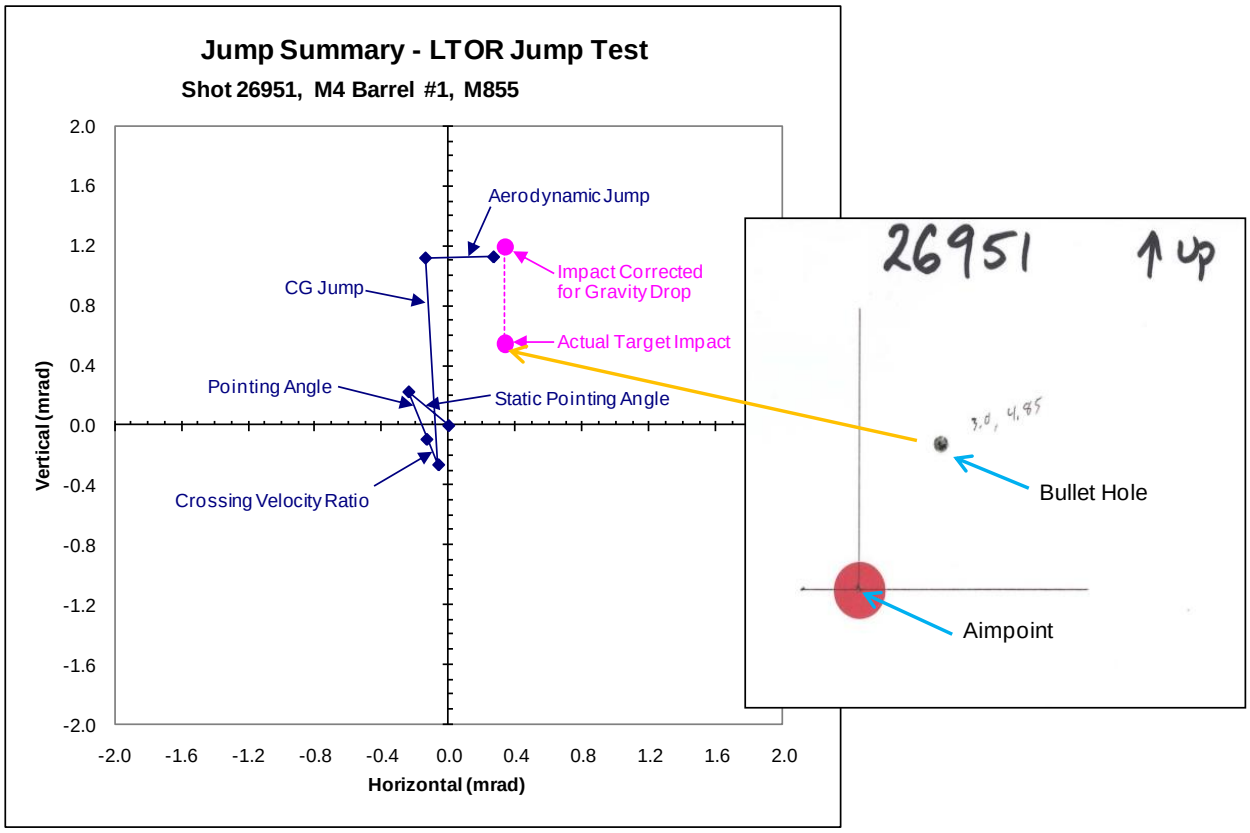

Figure 16. Jump component diagram with target impact adjustment, shot 26951.

4.3 Group Measurements

Jump components like those presented for example shot 26951 were obtained for all shots in each 10-shot group. The complete set of data facilitated a consideration of qualitative and statistical trends. The objective was to identify the most significant characteristics and contributions to jump dispersion.

Figure 17 is a composite of graphs showing the results of all 10 rounds for the M4 barrel no. 1 tests, grouped by jump components and total jump in the horizontal and vertical planes. The same scales are used in all six graphs, so the relative magnitudes and directions of jump components can be easily visualized. The horizontal and vertical group mean (i.e., average) and dispersion (i.e., standard deviations [SD]) of each jump component are given in parentheses (horizontal, vertical).

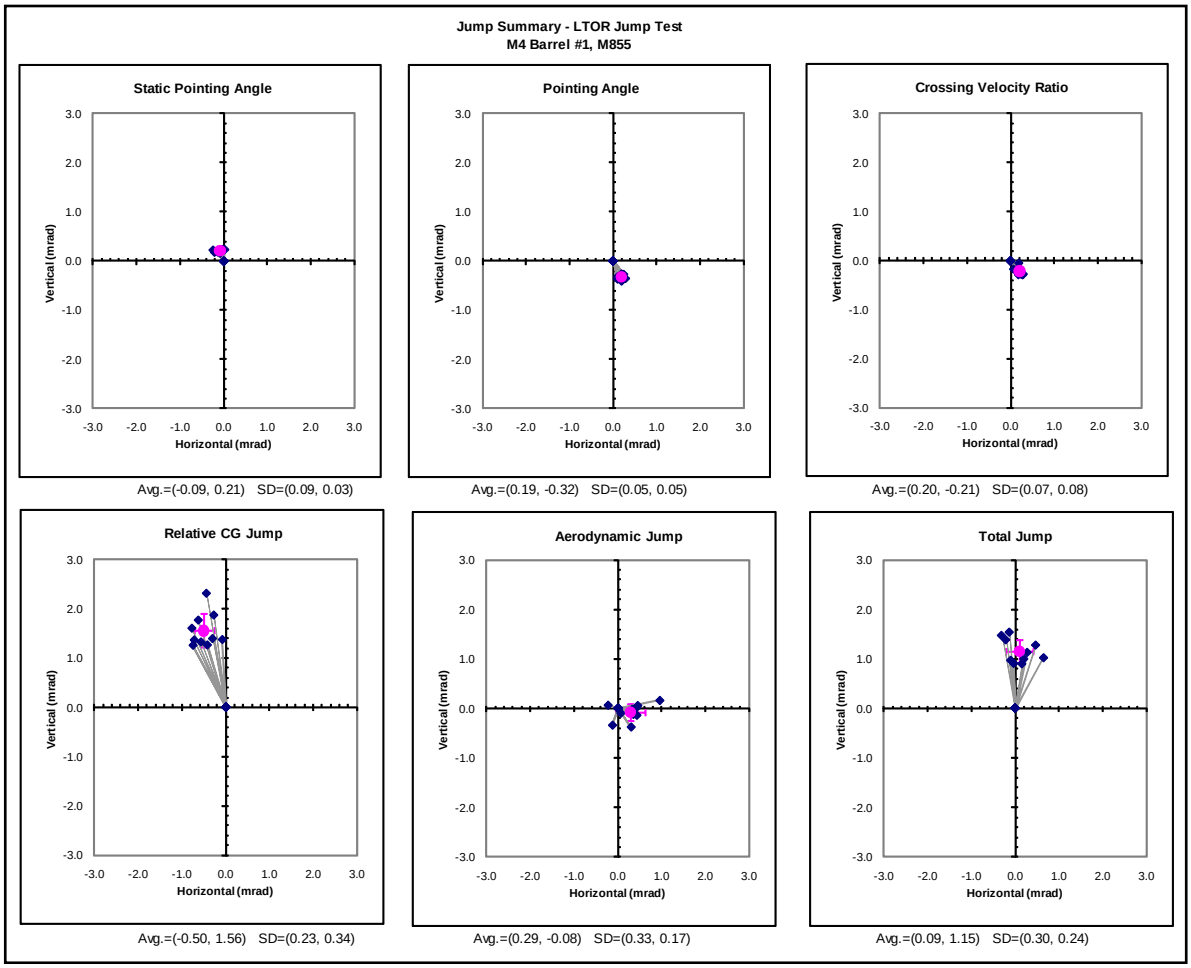

Figure 17. Basic jump components and total jump for 10-round group, M4 barrel no.1, M855.

4.4 Group Comparisons

In order to make comparisons between test configurations, the following figures and text show side by side composite results for individual jump components for the four different configurations. The first three figures show gun dynamics components on an expended scale, since as can be seen in figure 17, these jump components are significantly smaller than the other components.

Figure 18 shows the composite static pointing angle jump components for the four test configurations. This jump component shows barrel motion between the time the barrel is boresighted and the trigger is pulled. This motion was attributed to several factors. First, the weight of the borescope was sufficient to deflect the 5.56-mm barrel by a significant amount. Once the borescope was removed, the muzzle was no longer pointed at the aimpoint but was pointed above it. This factor is evident in the upward bias of the M4 configurations. Second, the attachment of the gun barrel to the receiver for the M4 weapon is relatively loose. This is usually not an issue since the gun sights are attached directly to the barrel itself. However, when jump testing, it is possible for the barrel to shift when a round is chambered. At that point it would be unsafe and irresponsible to bore-sight the gun.

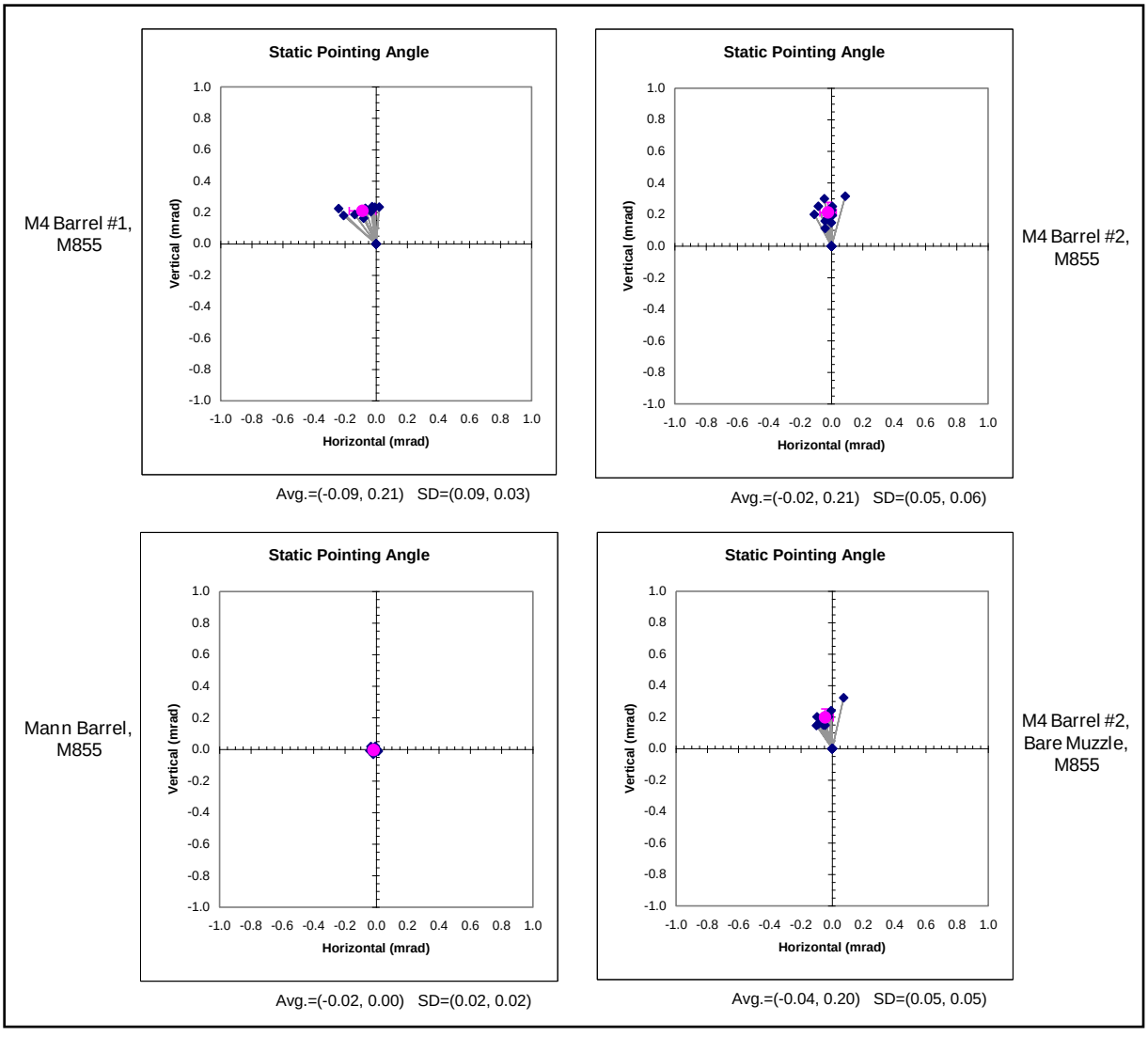

Figure 18. Static pointing angle jump component, expanded scale.

Neither of these two effects come into play with the Mann barrel. The barrel is rigid enough that the weight of the borescope does not deflect it, and the mounting is tighter so there is minimal motion while loading. This difference is reflected in figure 18 in that there is negligible static pointing angle jump for the Mann barrel.

The main significance of this jump component is to emphasize the fact that this initial (pre-shot) muzzle motion has been accounted for.

The pointing angle jump component is shown figure 19. This component indicates where the gun muzzle is pointing at the instant of shot exit. The Mann barrel again exhibits negligible response. There are some significant differences between the other three (M4) cases. Barrels no. 1 and no. 2 both show a similar downward bias, but barrel no. 1 has more of a bias toward the right. This difference is most likely due to manufacturing differences between the barrels (e.g., centerline profiles).

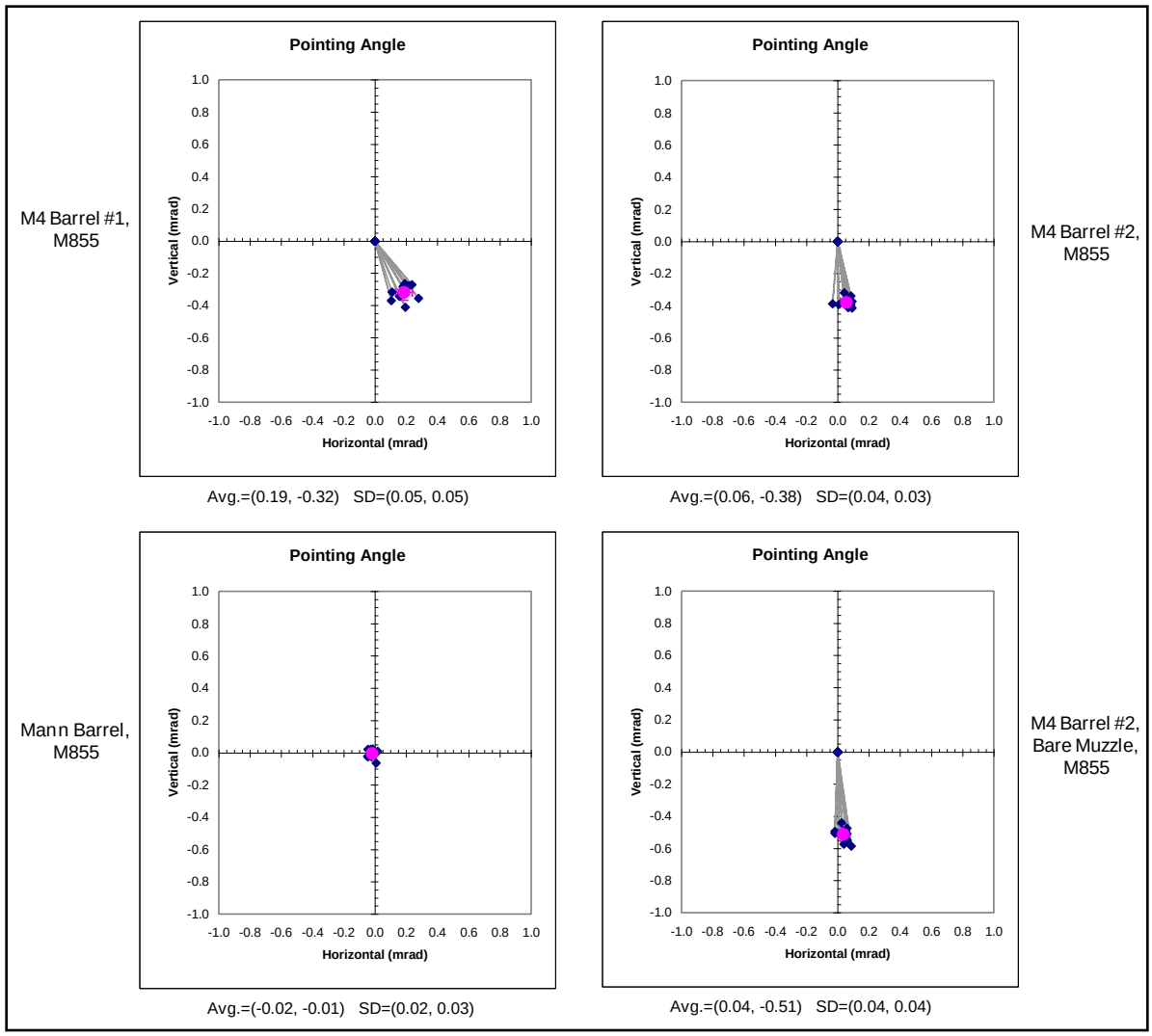

Figure 19. Pointing angle jump component, expanded scale.

Comparison of the two barrel no. 2 cases, with and without the compensator, shows a slightly more downward bias when the compensator is removed. One explanation for this would be a difference in the gun dynamics due to the removal of the mass of the compensator.

Figure 20 shows the crossing velocity ratio jump component. This again illustrates a difference in gun dynamics for barrel no. 2, with and without the compensator. The Mann barrel shows minimal motion.

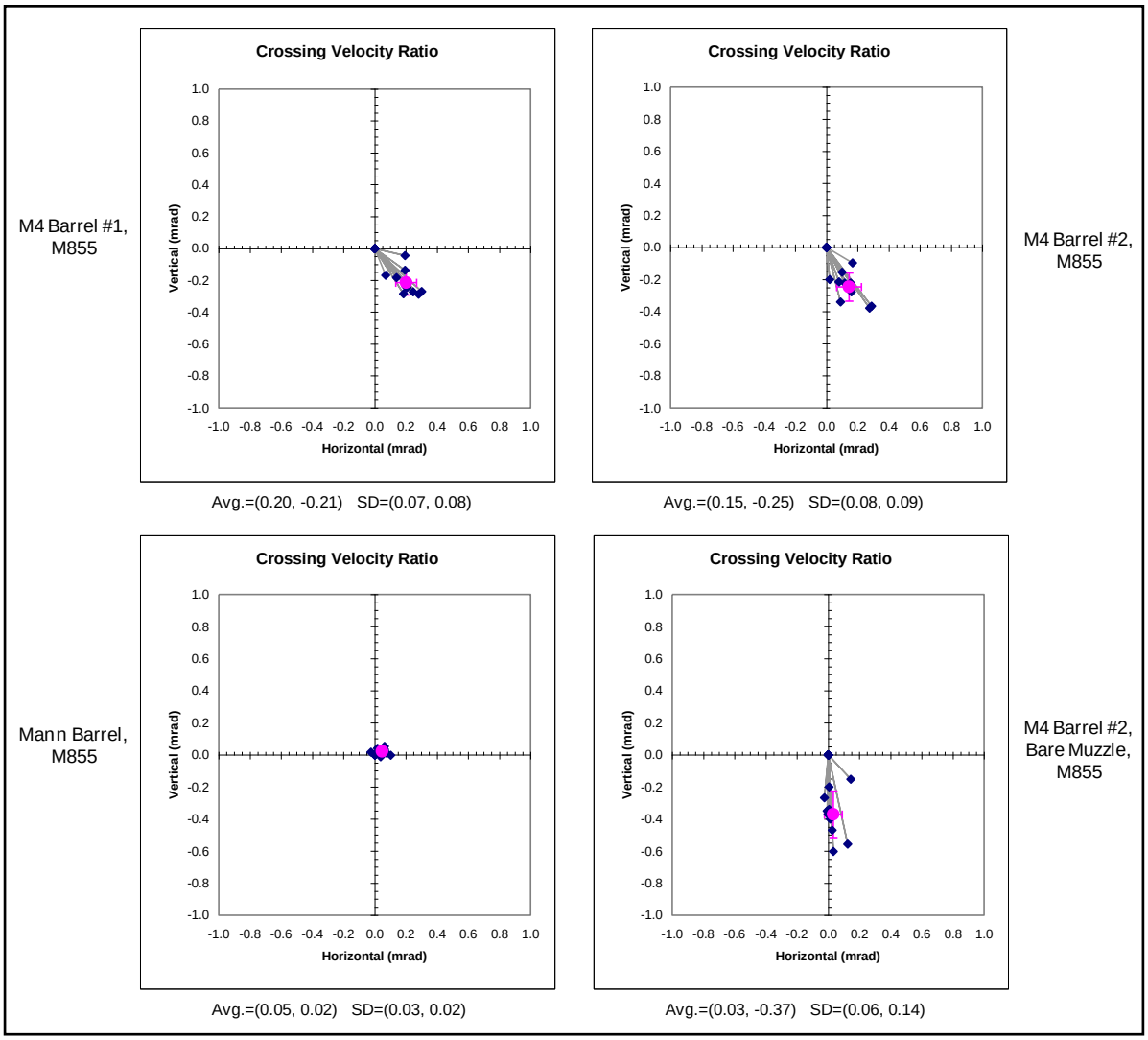

Figure 20. Crossing velocity ratio jump component, expanded scale.

Figure 21 shows the relative CG jump component for the four configurations. Relative CG jump indicates which direction the projectile CG is heading relative to where the gun barrel would have it go due to the pointing angle and crossing velocity ratio. For this component, there are slight differences between M4 barrels no. 1 and no. 2, with no. 1 biased up and to the left and no. 2 biased up and slightly right. Comparison of M4 barrel no. 2 with and without the compensator shows that there is a significant increase in upward CG motion when the compensator is in place. This will be discussed in more detail later.

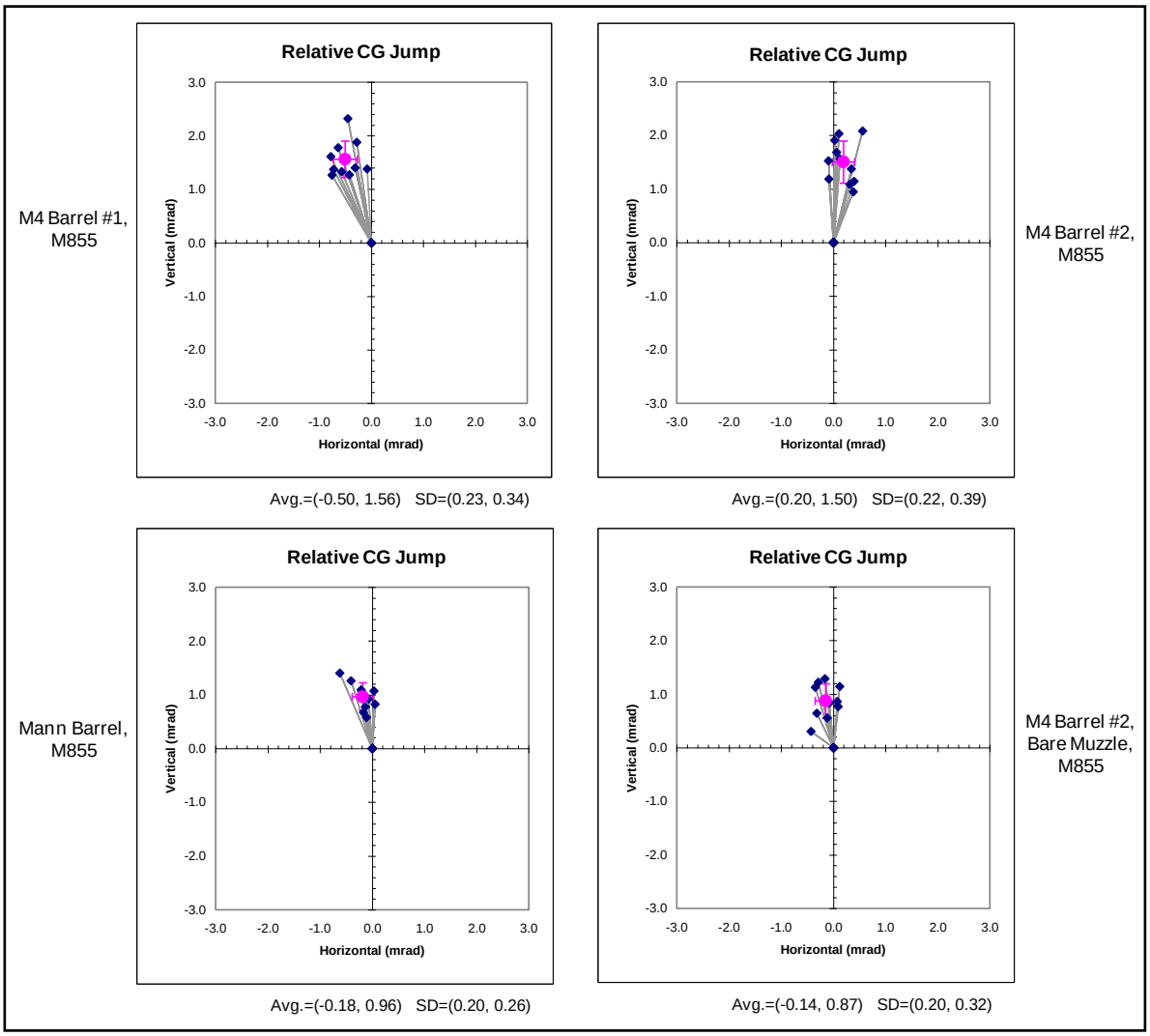

Figure 21. Relative CG jump component.

The relative CG jump for the Mann barrel is similar to that of the M4 barrel no. 2 bare muzzle case, indicating this component may be driven by the compensator.

The absolute CG jump component is shown in figure 22. Absolute CG jump is the trajectory of the bullet CG after shot exit, relative to the LOF. In general, the trends are similar to the relative CG jump, with one notable exception. When comparing the M4 barrel no. 2 with and without the compensator, it is evident that there is minimal absolute CG jump for the bare muzzle case. Both the magnitude and standard deviation of this component are much lower when the compensator is not present. The magnitude decrease appears to be fortuitous, since removing the compensator increased the magnitudes of the gun dynamics jump components but decreased relative jump just enough that the magnitudes of these components offset each other. The standard deviation decrease cannot be readily explained.

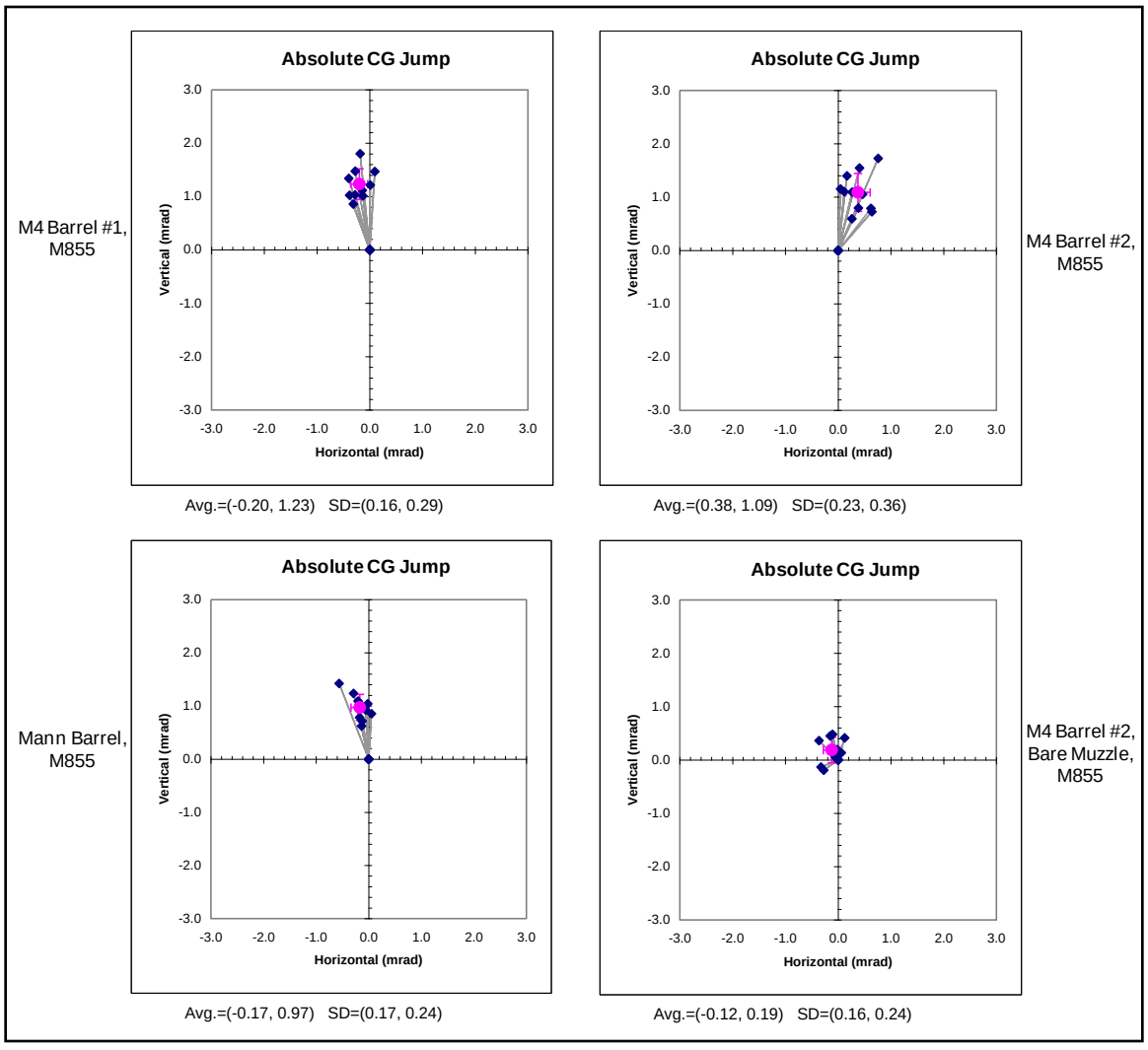

Figure 22. Absolute CG jump component.

Figure 23 shows the aerodynamic jump component for each of the four configurations. Aerodynamic jump is the angle between the projectile's downrange trajectory and the initial trajectory angle, and is the result of the integrated effect of aerodynamic lift due to the yawing motion of the projectile. There are some differences in the SDs for the different configurations.

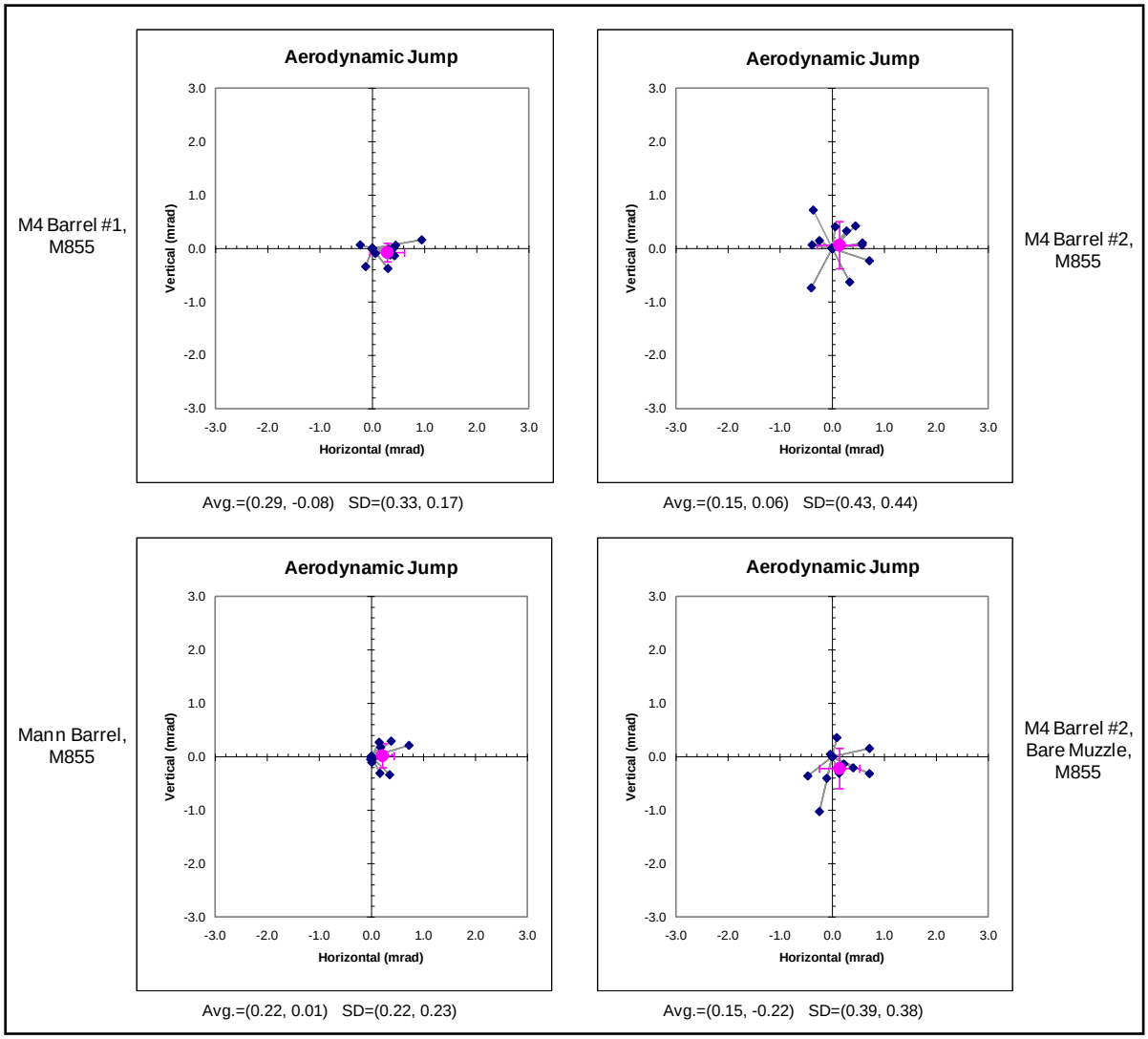

Figure 23. Aerodynamic jump component.

The Mann barrel has the lowest dispersion, followed by M4 barrel no. 1. M4 barrel no. 2 has the largest SDs both with and without the compensator. Large aerodynamic jump dispersion is indicative of inconsistently imparted initial angular projectile motion.

Total jump is shown in figure 24. Total jump is the vector sum of all of the jump components and is indicative of the impact on the target, both in terms of bias and dispersion. When comparing M4 barrels no. 1 and no. 2, there is a noticeable bias to the right for barrel no. 2. A more interesting comparison is M4 barrel no. 2 with and without the compensator. When the compensator is removed, the total jump is essentially centered on the LOF.

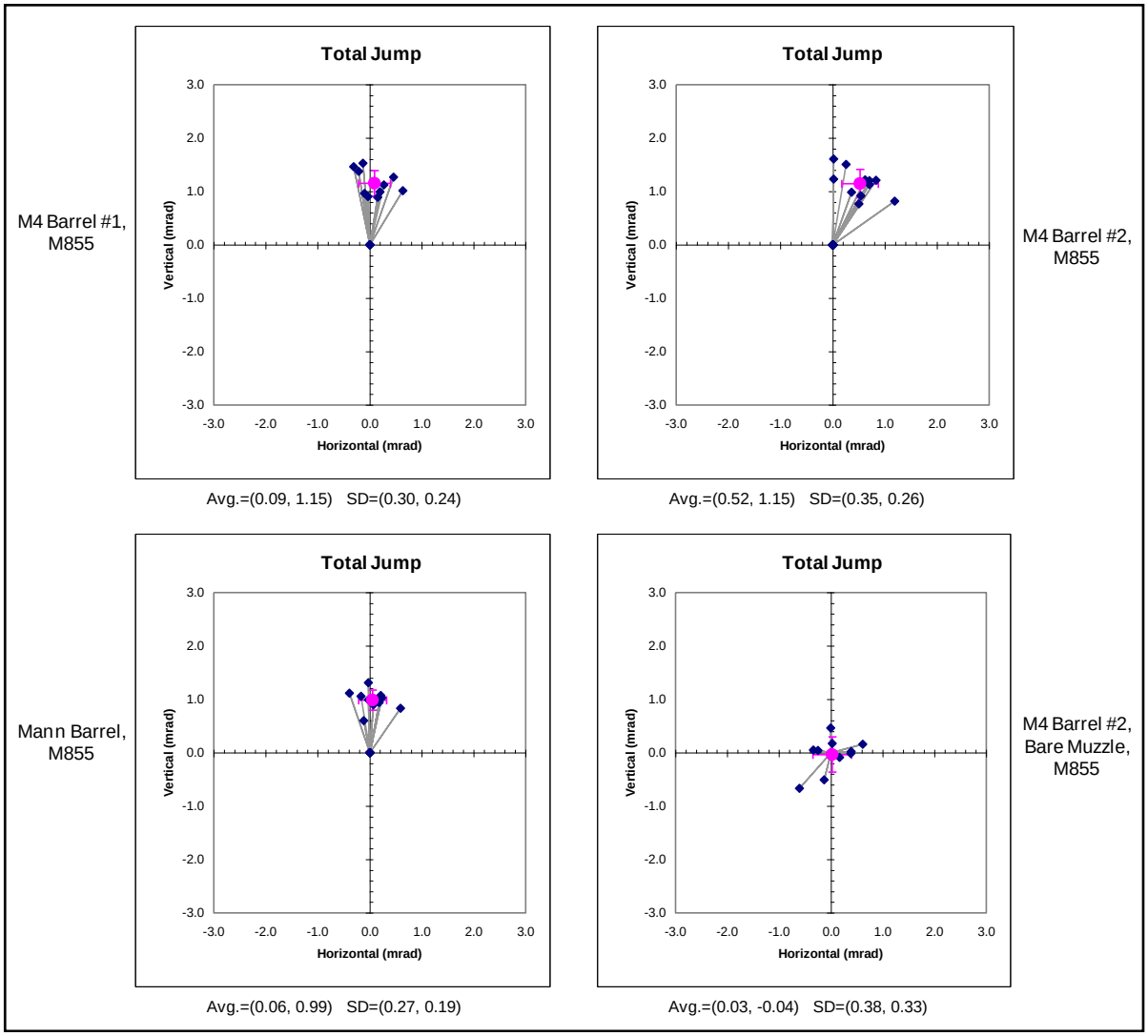

Figure 24. Total jump.

Table 2 lists the average horizontal and vertical jump component magnitudes for the four tested configurations.

Table 2. Horizontal and vertical jump component average magnitudes.

	Static Muzzle Jump	Pointing Angle Jump	Crossing Velocity Jump	Point Ang + Cross Vel	Absolute CG Jump	Relative CG Jump	Aero-dynamic Jump	Total Jump
M4, Barrel No. 1								
Horizontal	–0.088	0.187	0.202	0.389	–0.199	–0.499	0.293	0.094
Vertical	0.210	–0.320	–0.213	–0.534	1.235	1.558	–0.080	1.154
M4, Barrel No. 2								
Horizontal	–0.022	0.057	0.145	0.202	0.376	0.195	0.148	0.524
Vertical	0.213	–0.380	–0.247	–0.627	1.088	1.503	0.059	1.147
M4, Barrel No. 2, Bare Muzzle								
Horizontal	–0.045	0.037	0.033	0.070	–0.120	–0.145	0.146	0.026
Vertical	0.197	–0.514	–0.371	–0.885	0.186	0.874	–0.222	–0.036
Mann Barrel								
Horizontal	–0.016	–0.018	0.049	0.031	–0.167	–0.182	0.223	0.056
Vertical	–0.004	–0.007	0.021	0.013	0.974	0.965	0.012	0.986

4.4 Dispersion of Jump Components

Figure 25 displays bar charts showing the horizontal, vertical, and radial dispersions of the jump components for the four tested configurations. Radial dispersion (radial standard deviation [RSD]) is defined as the square root of the sum of the squares of the horizontal and vertical dispersions. The basic jump components are shown as solid bars; additional jump components (static pointing angle, pointing angle + crossing velocity, and absolute CG jump) are shown as striped bars. The charts clearly show the reduced level of gun dynamics dispersion for the Mann barrel, as well as component differences for the other configurations.

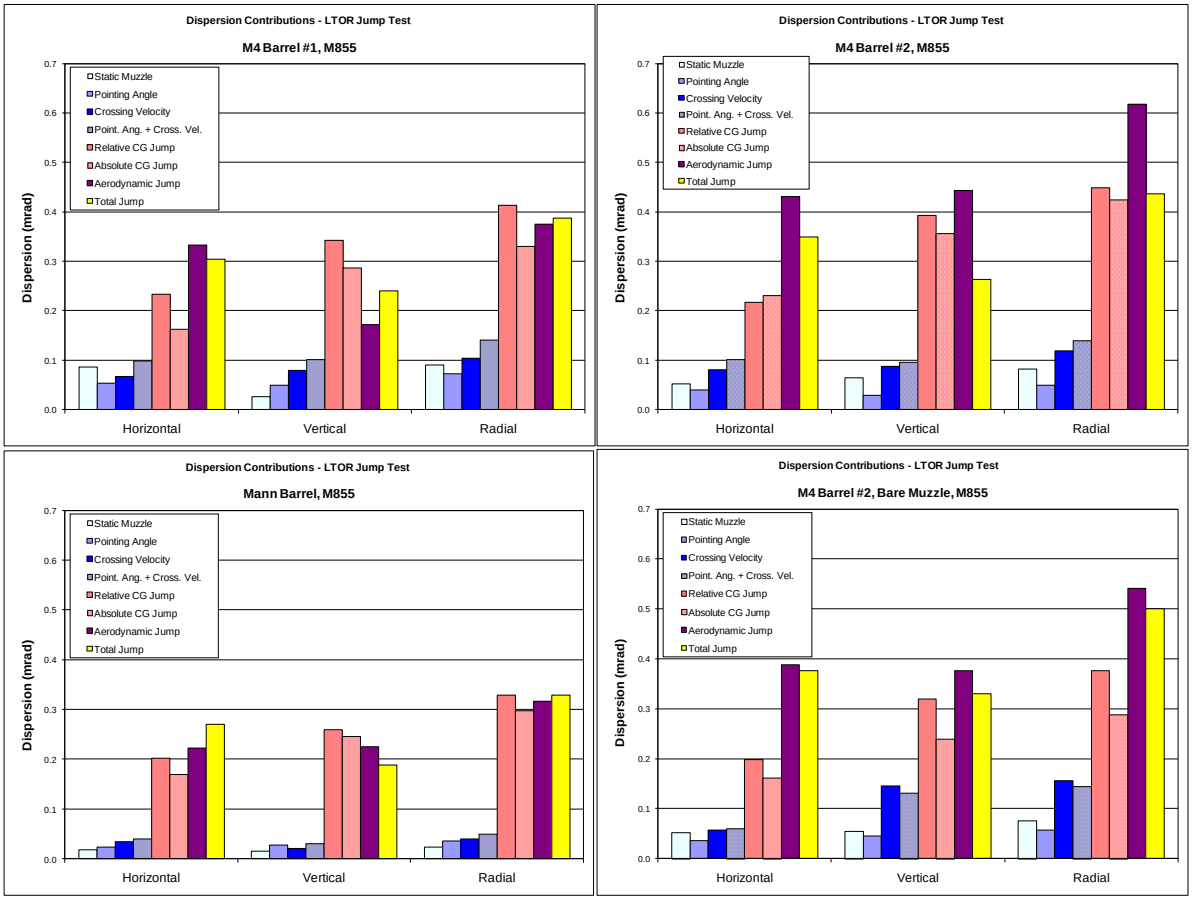

Figure 25. Dispersions of jump components and total jump.

Table 3 lists the horizontal, vertical and radial jump component dispersions (standard deviations) for the four tested configurations.

Table 3. Horizontal, vertical, and radial jump component dispersions.

	Static Muzzle Jump	Pointing Angle Jump	Crossing Velocity Jump	Point Ang + Cross Vel	Absolute CG Jump	Relative CG jump	Aero-dynamic Jump	Total Jump
M4, Barrel No. 1								
Horizontal	0.085	0.054	0.066	0.098	0.163	0.233	0.333	0.305
Vertical	0.026	0.048	0.079	0.100	0.287	0.342	0.172	0.240
Radial	0.089	0.072	0.103	0.140	0.329	0.414	0.374	0.388
M4, Barrel No. 2								
Horizontal	0.052	0.040	0.080	0.101	0.230	0.217	0.431	0.349
Vertical	0.063	0.028	0.088	0.095	0.356	0.393	0.443	0.263
Radial	0.082	0.049	0.118	0.139	0.424	0.449	0.618	0.437
M4, Barrel No. 2, Bare Muzzle								
Horizontal	0.052	0.035	0.057	0.059	0.160	0.198	0.388	0.376
Vertical	0.054	0.045	0.145	0.131	0.238	0.319	0.376	0.329
Radial	0.075	0.057	0.156	0.143	0.287	0.376	0.541	0.500
Mann Barrel								
Horizontal	0.017	0.023	0.034	0.039	0.169	0.202	0.222	0.269
Vertical	0.015	0.028	0.020	0.030	0.245	0.259	0.225	0.188
Radial	0.023	0.036	0.039	0.049	0.297	0.328	0.316	0.328

The largest jump component dispersion contributors for all four configurations are the relative CG jump and the aerodynamic jump. The magnitudes of the dispersions of the gun dynamics components are on the order of 25% of the larger components.

4.5 Negative Correlations

Figure 25 also shows that the total jump dispersion is smaller than the square root of the sum of the squares of the individual jump components. Furthermore, the dispersions of the relative CG jump components and/or the aerodynamic jump components are larger than the total jump dispersions in most cases. As a result, interactions (i.e., correlations) must exist between some or all jump components. Analysis was conducted to identify strong interactions among the basic jump components and among the additional jump components introduced earlier in the report. Strong interactions were identified between relative CG jump and aerodynamic jump.

Figures 26–29 show correlations between relative CG jump and aerodynamic jump for the four test cases. For each case, four correlations are shown for the different combinations of horizontal and vertical components. For barrel no. 2 with the compensator (figure 27), negative correlations exist for all four cases, with the strongest being between the vertical components. What this means is that when the relative CG jump increases, there is a corresponding decrease in the aerodynamic jump.

When comparing barrel no. 1 (figure 26) with barrel no. 2 (figure 27), the most significant difference is that barrel no. 1 shows a weak positive correlation for the combination of horizontal relative CG jump and vertical aerodynamic jump, while barrel no. 2 shows a weak negative correlation. This difference in sign can be attributed to the poor quality of this correlation in both cases. Differences between barrel no. 2 and barrel no. 2 bare muzzle (figures 27 and 28) will be discussed in detail later. The Mann barrel correlations (figure 29) look somewhat different, with a strong positive correlation for the combination of horizontal relative CG jump and vertical aerodynamic jump. Most likely this is due to the significantly different barrel and mount geometry.

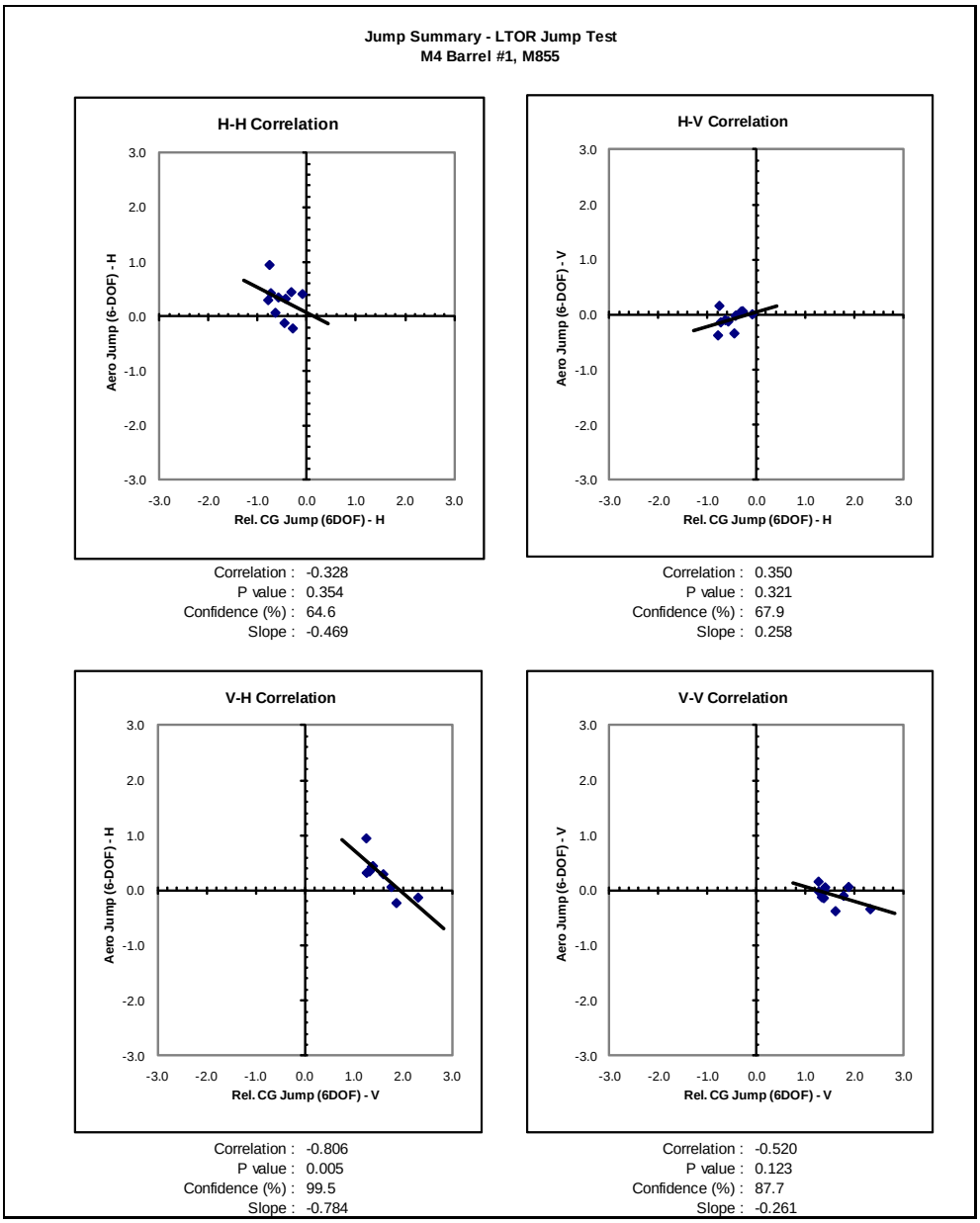

Figure 26. Correlations between relative CG jump and aerodynamic jump for barrel no. 1.

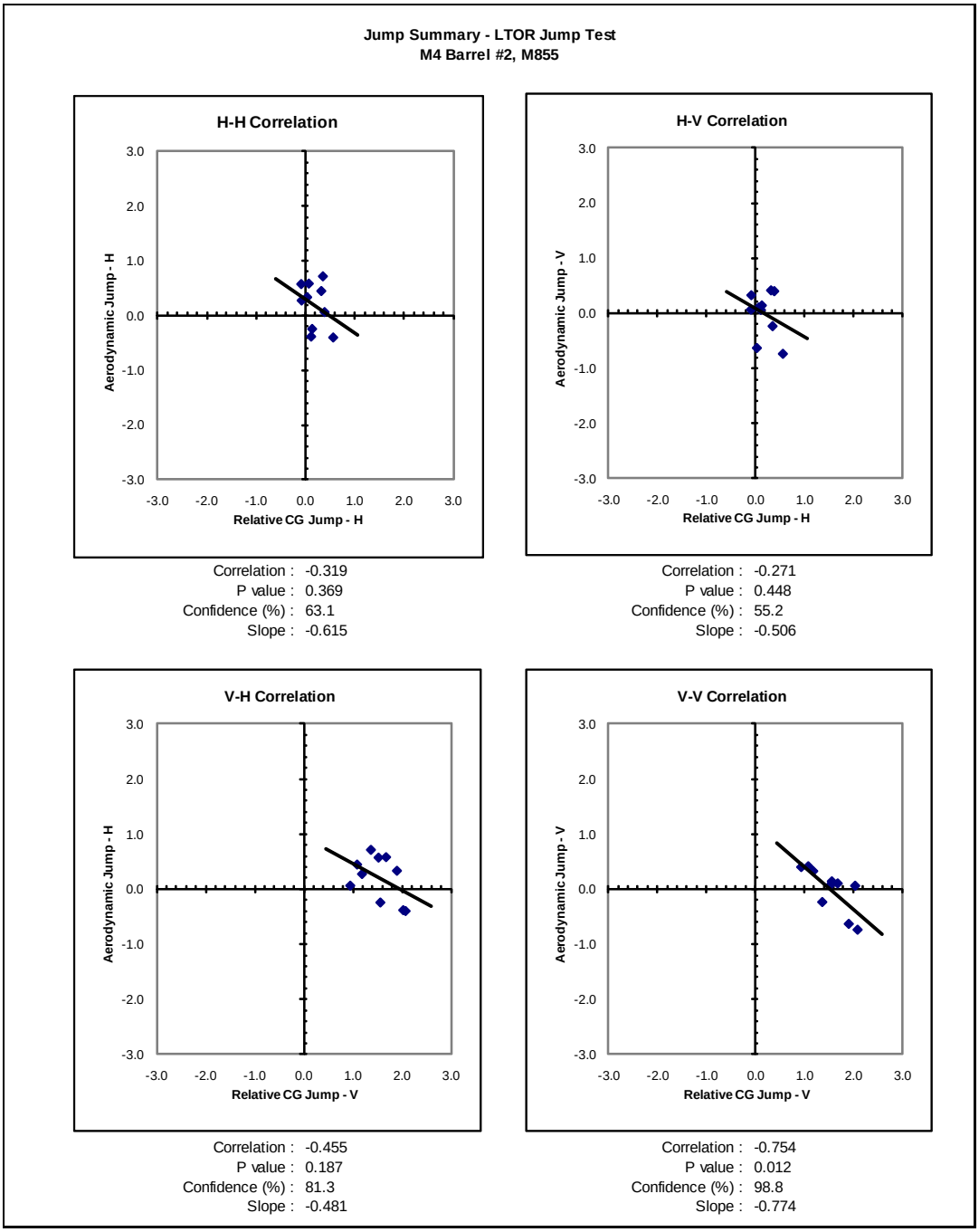

Figure 27. Correlations between relative CG jump and aerodynamic jump for barrel no. 2.

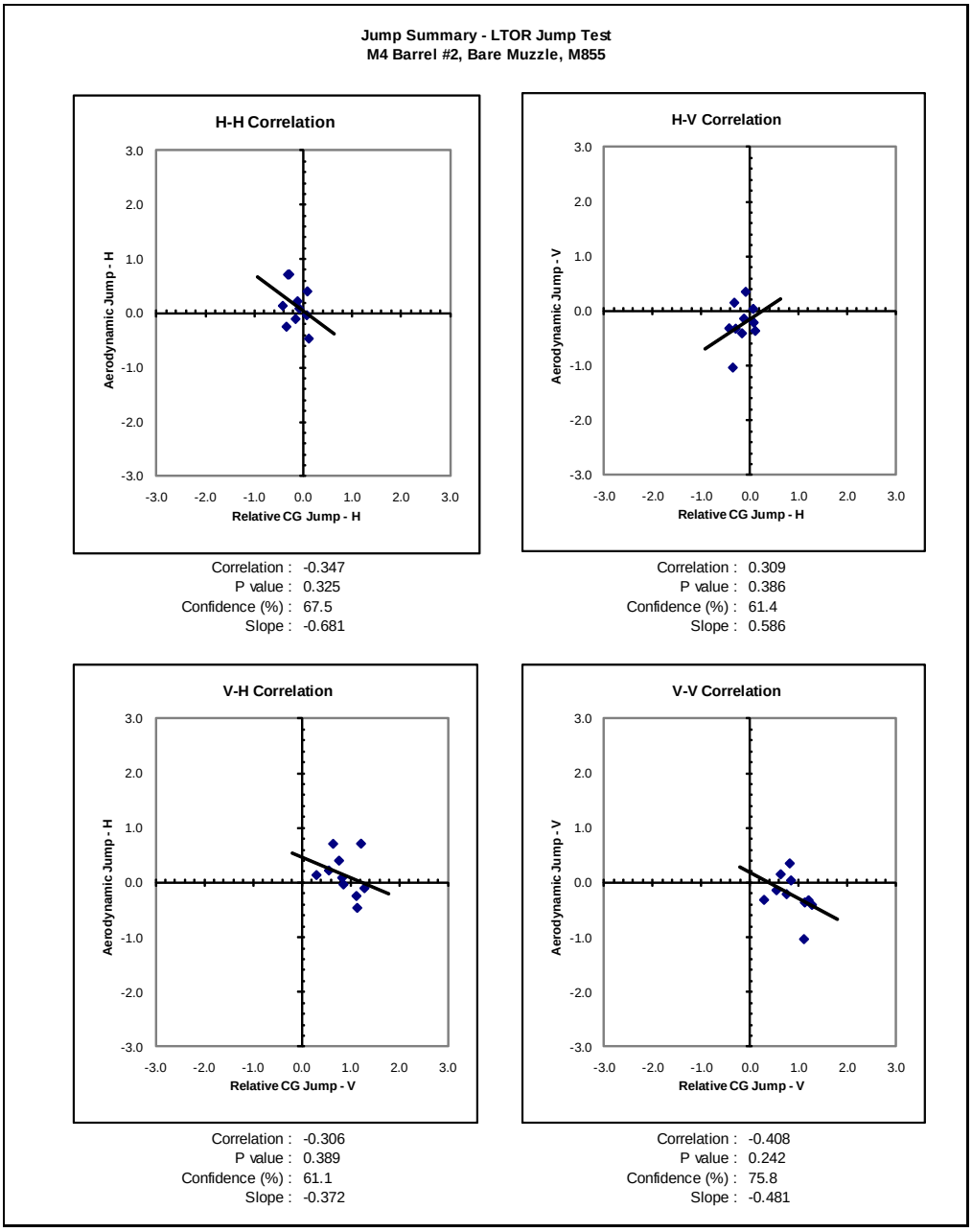

Figure 28. Correlations between relative CG jump and aerodynamic jump for barrel no. 2 bare muzzle.

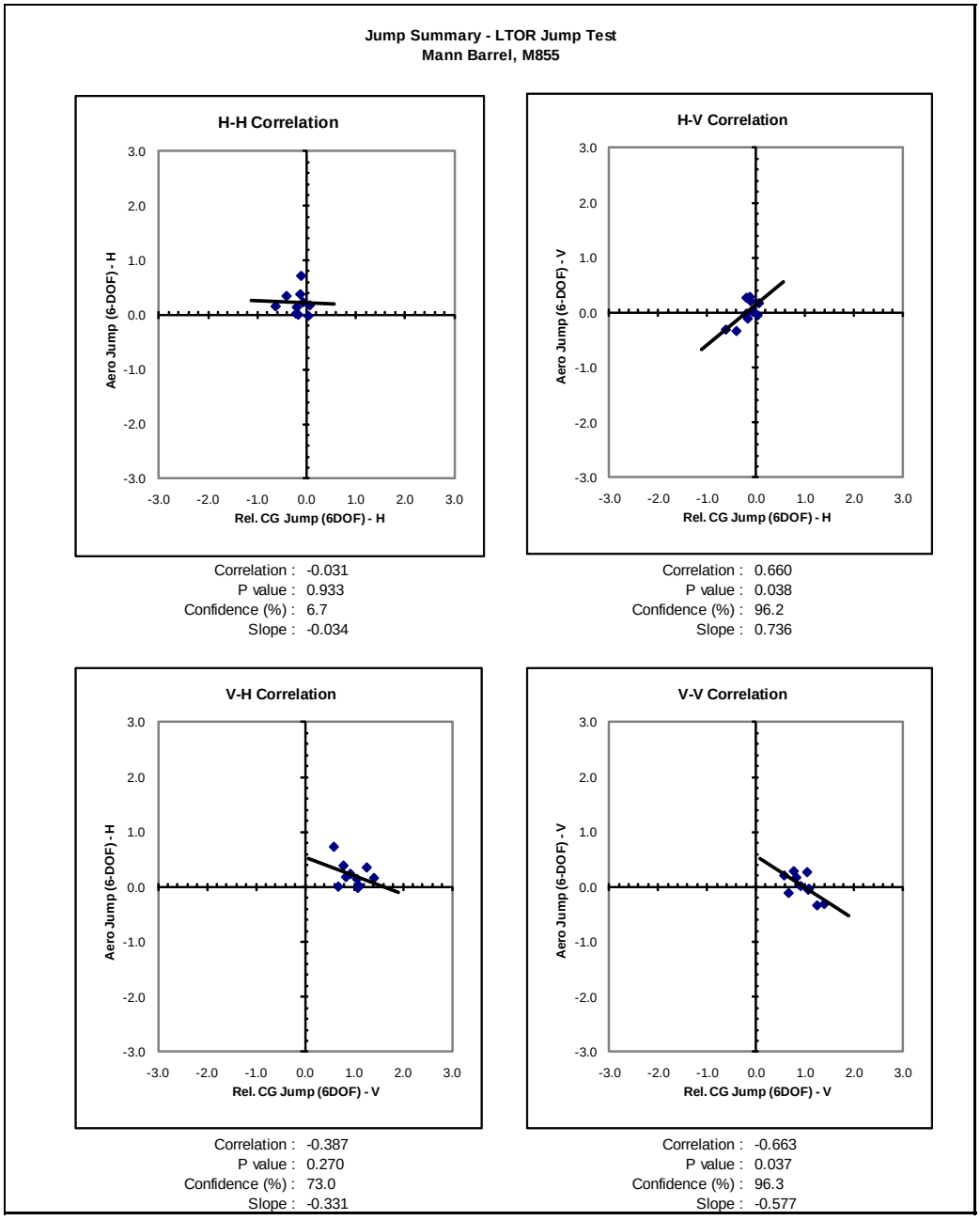

Figure 29. Correlations between relative CG jump and aerodynamic jump for Mann barrel.

4.6 Muzzle Compensator Effect

The fact that the muzzle compensator has an effect on the launch dynamics is evident from the jump component plots. This difference is most pronounced in the CG jump and total jump components, as can be seen in figures 21, 22, and 24. When the compensator is present, there is a pronounced upward bias in the CG jump and total jump. This effect can be explained by an examination of the compensator geometry.

Figure 30 shows a picture of the compensator attached to a weapon. It can clearly be seen that the compensator is vertically asymmetric. The purpose of the compensator is to mitigate muzzle climb when the weapon is fired in automatic mode by venting gun gases in the vertical direction. This asymmetric muzzle flow field also affects the flight of the bullet and explains the upward bias in the trajectory. The gun gases will vent from the top of the compensator, resulting in a pressure difference in the vertical direction, with higher pressure gas below the bullet. These gases exert an upward force on the bullet, resulting in upwards deviation of the trajectory.

Figure 30. Muzzle compensator with asymmetric venting.

A trajectory that is deflected upwards is not necessarily bad—it can be compensated for with sight adjustments. A more significant consideration is the effect of the compensator on dispersion. Examinations of figures 24 and 25 and table 3 show that the total dispersion was lower for the M4 barrel no. 2 group with the compensator than it was for the bare muzzle case. This was true even though component dispersions for CG jump and aerodynamic jump tended to be larger for the compensator configuration. This can only happen if there are larger negative correlations when the compensator is present.

Figure 31 shows a side by side comparison of correlations in the vertical plane between relative CG jump and aerodynamic jump for M4 barrel no. 2 with and without the compensator. When the compensator is present, the negative correlation is indeed much stronger.

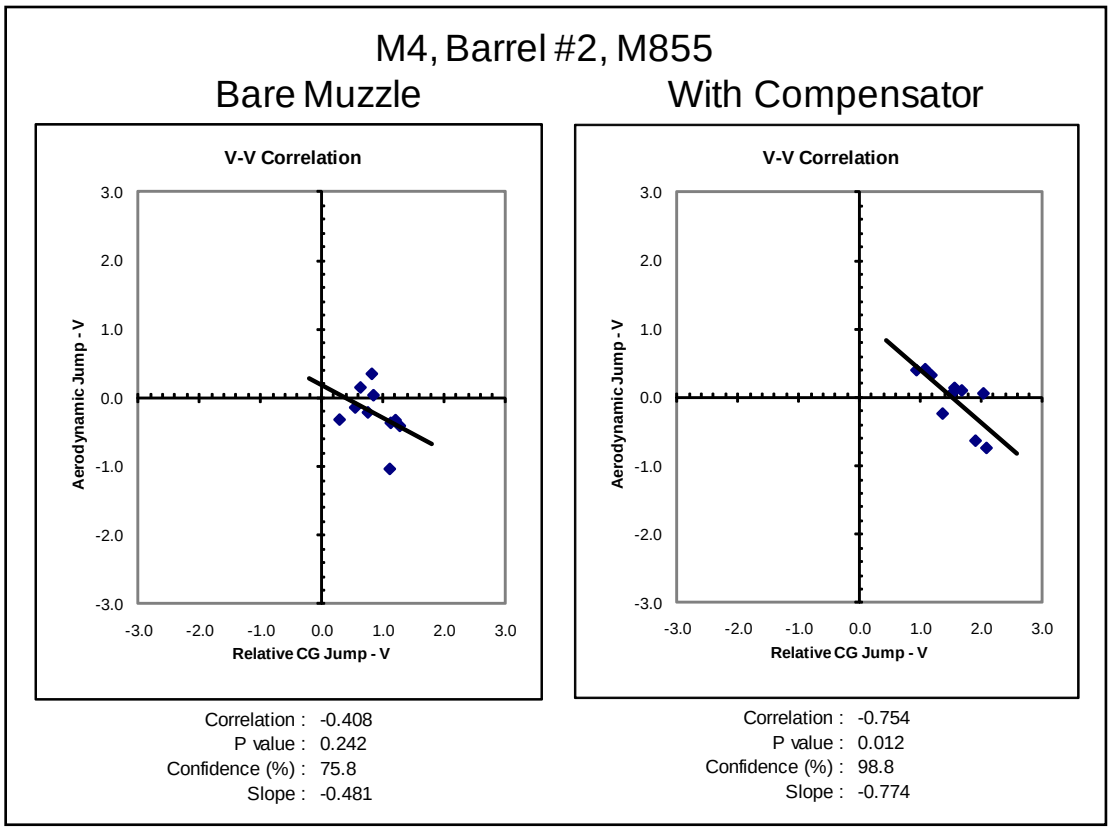

Figure 31. Comparison of correlations for M4, barrel no. 2 with and without compensator.

A summary of the observed differences when the compensator is installed follows:

- The magnitude of the vertical component of CG jump increases substantially (going from 0.87 to 1.50 mrad).
- The magnitude of the total jump increases dramatically (total radial jump increases from 0.05 to 1.26 mrad).
- There is a small decrease in the dispersion of the gun dynamics. Pointing angle RSD decreases from 0.06 to 0.05 mrad and crossing velocity RSD decreases from 0.16 to 0.12 mrad.
- Negative correlations between jump components are strengthened.
- There is a slight decrease in total dispersion, mainly in the vertical plane. Total dispersion (RSD) decreases from 0.50 to 0.44 mrad, and vertical dispersion decreases from 0.33 to 0.26 mrad.

Although the compensator is designed to improve performance when firing in automatic, the overall net effect of having the compensator installed seems to be positive even when firing in single shot mode, in that the dispersion of the weapon is reduced.

4.7 Mann Barrel Differences

The Mann barrel has a much thicker wall than the standard M4 barrel, and the Mann barrel mount is a much more rigid mount than the M4 weapon. The main result of these differences is a significant reduction in the motion of the gun barrel during firing. This reduces both the magnitudes and standard deviations of the gun dynamics jump components, as can be seen in figures 19, 20, and 25, and also in tables 2 and 3.

There is also a decrease in the dispersions of the CG jump and aerodynamic jump components, most likely due to the fact that lower gun motion will impart smaller linear and angular impulses to the bullet.

The most significant results when comparing the Mann barrel with the average of M4 barrels no. 1 and no. 2, and with M4 barrel no. 2, bare muzzle are:

- The magnitude of the gun dynamics jump components is reduced dramatically. Muzzle pointing angle (radial) is reduced to 0.2 mrad from 0.38 (average of 1 and 2) or 0.51 (no. 2 bare muzzle). Crossing velocity (radial) is reduced to 0.05 mrad from 0.29 (average of 1 and 2) or 0.37 (no. 2 bare muzzle).
- The dispersion of the gun dynamics jump components is reduced. Muzzle pointing angle (RSD) is reduced to 0.04 mrad from 0.06 (average of 1 and 2) or 0.06 (no. 2 bare muzzle). Crossing velocity (RSD) is reduced to 0.04 mrad from 0.11 (average of 1 and 2) or 0.16 (no. 2 bare muzzle).
- The total jump dispersion RSD is reduced to 0.33 mrad from 0.42 (average of 1 and 2) or 0.50 (no. 2 bare muzzle).

The significance of these differences is that care must be taken when using a Mann barrel to evaluate ammunition performance. There would be some potential benefit when comparing performance of ammunition lots or ammunition types in that the contributions of gun effects would be minimized. However, Mann barrel test results cannot be used for assessing system performance since it is a significantly different launch environment from the M4 weapon.

5. Summary

Jump characterization of the M855 projectile fired from the M4 weapon and from a Mann barrel was performed to quantify sources of error that comprise the total accuracy of the system. Forty total rounds were fired from four different configurations. Two of the configurations attempted to simulate shoulder firing of a standard M4 with two different barrels. The third configuration was identical except that the muzzle compensator was removed. The final configuration used a heavy wall Mann barrel in a mount that restricted lateral gun tube motion.

The firings were conducted under ambient conditions. The average launch velocity was 859.4 m/s, with a standard deviation of 5.7 m/s. The lowest measured launch velocity was 849.7 m/s; the highest was 873.5 m/s.

The magnitudes of the CG jump and aerodynamic jump components were significantly larger than the muzzle motion components. Removal of the compensator resulted in slightly increased muzzle motion, which can be attributed to removal of mass from the muzzle. As expected, the Mann barrel exhibited drastically reduced muzzle motion.

The largest jump component dispersion contributors for all four configurations were the relative CG jump and the aerodynamic jump. The magnitudes of the dispersions of the gun dynamics components were on the order of 25% of the larger components. The dispersions of the relative CG jump components and/or the aerodynamic jump components were larger than the total jump dispersions in most cases, indicating that negative correlations must exist between some or all jump components. Strong interactions were identified between relative CG jump and aerodynamic jump, which served to reduce the total jump.

There were minimal differences between the two different standard barrels (M4 barrel no. 1 and M4 barrel no. 2).

The overall effect of the compensator was positive, in that it resulted in lower total jump dispersion. With the compensator in place, there was an increase in CG jump in the vertical plane and an increase in dispersion of vertical CG jump and vertical aerodynamic jump. The overall decrease in total jump dispersion with the compensator in place was due to strengthened negative correlations.

For the Mann barrel, both the magnitudes and standard deviations of the gun dynamics jump components were reduced. There was also a decrease in the dispersions of the CG jump and aerodynamic jump components, most likely due to the fact that lower gun motion imparted smaller linear and angular impulses to the bullet. As a result, the total jump dispersion for the Mann barrel was also lower. The implication is that the Mann barrel provides a significantly different dynamic launch environment than the standard M4 weapon. This must be taken into consideration when using Mann barrels to evaluate ammunition performance.

6. References

1. Celmins, I. *Jump Component Measurement Methodology for Small-Caliber, Spin-Stabilized Ammunition*; ARL-TR-4259; U.S. Army Research Laboratory: Aberdeen Proving Ground, MD, September 2007.

2. Bornstein, J. A.; Celmins, I.; Plostins, P.; Schmidt, E. M. *Techniques for the Measurement of Tank Cannon Jump*; BRL-MR-3715; U.S. Army Ballistics Research Laboratory: Aberdeen Proving Ground, MD, December 1988.

3. Braun, W. F. *The Free Flight Aerodynamics Range*; BRL Report No. 1048; U.S. Army Ballistics Research Laboratories: Aberdeen Proving Ground, MD, July 1958.

4. Bornstein, J. A.; Haug, B. T. *Gun Dynamics Measurements for Tank Gun Systems*; BRL-MR-3688; U.S. Army Ballistics Research Laboratory: Aberdeen Proving Ground, MD, July 1988.

5. Arrow Tech Associates, *ARFDAS: Ballistic Range Data Analysis System; User and Technical Manual,* South Burlington, VT, May 1997.

6. McCoy, R. L. *Modern Exterior Ballistics*; Schiffer Publishing Ltd.: Atglen, PA, 1999.

7. Murphy, C. H. *Free Flight Motion of Symmetric Missiles*; BRL-TR-1216; U.S. Army Ballistics Research Laboratory: Aberdeen Proving Ground, MD, December 1963.

NO. OF COPIES	ORGANIZATION
1 (PDF only)	DEFENSE TECHNICAL INFORMATION CTR DTIC OCA 8725 JOHN J KINGMAN RD STE 0944 FORT BELVOIR VA 22060-6218
1	DIRECTOR US ARMY RESEARCH LAB IMNE ALC HRR 2800 POWDER MILL RD ADELPHI MD 20783-1197
1	DIRECTOR US ARMY RESEARCH LAB RDRL CIM L 2800 POWDER MILL RD ADELPHI MD 20783-1197
1	DIRECTOR US ARMY RESEARCH LAB RDRL CIM P 2800 POWDER MILL RD ADELPHI MD 20783-1197
1	DIRECTOR US ARMY RESEARCH LAB RDRL D 2800 POWDER MILL RD ADELPHI MD 20783-1197
	ABERDEEN PROVING GROUND
1	DIR USARL RDRL CIM G (BLDG 4600)

NO. OF COPIES	ORGANIZATION
1	COMMANDER US ARMY MATL CMD AMXMI INT 9301 CHAPEK RD FORT BELVOIR VA 22060-5527
1	US ARMY TACOM ARDEC CCAC AMSRD AAR MEM J G FLEMING BLDG 65N PICATINNY ARSENAL NJ 07806-5000
1	US ARMY TACOM ARDEC ASIC PRGM INTEGRATION OFC J A RESCH BLDG 1 PICATINNY ARSENAL NJ 07801
1	US ARMY TACOM ARDEC AMSRD AR CCL C S SPICKERT-FULTON BLDG 65 N PICATINNY ARSENAL NJ 07806-5000
1	PRODUCT MGR SML AND ME CAL AMMO SFAE AMO MAS SMC LTC WOODS BLDG 354 PICATINNY ARSENAL NJ 07806-5000
4	PM ARMS SFAE AMO MAS SMC R KOWALSKI F HANZL P RIGGS J LUCID BLDG 354 PICATINNY ARSENAL NJ 07806-5000
1	US ARMY ARDEC AMSRD AAR AEM T M NICOLICH BLDG 65S PICATINNY ARSENAL NJ 07806-5000

NO. OF COPIES	ORGANIZATION
1	US ARMY ARDEC AMSRD AAR AEM L D VO BLDG 65 S PICATINNY ARSENAL NJ 07806-5000
1	US ARMY ARDEC AMSRD AAR AEM S S MUSALLI BLDG 65S PICATINNY ARSENAL NJ 07806-5000
1	US ARMY ARDEC AMSRD AAR EMI R CARR BLDG 65N PICATINNY ARSENAL NJ 07806-5000
2	US ARMY ARDEC AMSRD AAR CCL B M MINISI K RUSSEL BLDG 65N PICATINNY ARSENAL NJ 07806-5000
2	US ARMY ARDEC AMSRD AAR AIJ K SPIEGEL BLDG 65 PICATINNY ARSENAL NJ 07806-5000
4	US ARMY ARDEC AMSRD AAR AEM I J MIDDLETON G DEROSA M VOLKMANN A ISMAILOV BLDG 65N PICATINNY ARSENAL NJ 07806-5000

NO. OF COPIES ORGANIZATION

1 US ARMY ARDEC
RDAR MEF E
D CARLUCCI
BLDG 1
PICATINNY ARSENAL NJ
07806-5000

3 COMMANDER
US ARMY RDECOM ARDEC
RDAR MEM A
C LIVECCHIA
J GRAU
B WONG
BLDG 94
PICATINNY ARSENAL NJ 07806-5000

6 COMMANDER
US ARMY RDECOM ARDEC
RDAR MEM A
G MALEJKO
E VAZQUEZ
W TOLEDO
W KOENIG
S CHUNG
T RECCHIA
BLDG 94S
PICATINNY ARSENAL NJ 07806-5000

5 COMMANDER
US ARMY RDECOM ARDEC
RDAR MEM A
A FARINA
L YEE
R TROHANOWSKY
S HAN
C WILSON
BLDG 94
PICATINNY ARSENAL NJ 07806-5000

1 COMMANDER
US ARMY RDECOM ARDEC
RDAR MEM
E LOGSDON
BLDG 65
PICATINNY ARSENAL NJ 07806-5000

1 COMMANDER
US ARMY ARDEC
AMSTA AAR AEM I
M NICKOLICH
BLDG 65 N
PICATINNY ARSENAL NJ 07806-5000

NO. OF COPIES ORGANIZATION

1 ALLIANT TECHSYSTEMS INC
R DOHRN
MN07 MN14
4700 NATHAN LN
PLYMOUTH MN 55442

1 ATK
M JANTSCHER
MN07 LW54
4700 NATHAN LN N
PLYMOUTH MN 55442

5 ATK LAKE CITY
SMALL CALIBER AMMUN
LAKE CITY ARMY AMMUN PLANT
D MANSFIELD
PO BOX 1000
INDEPENDENCE MO 64051-1000

2 ATK LAKE CITY
LAKE CITY ARMY AMMUN PLANT
SMALL CALIBER AMMUN
J WESTBROOK
M WOLFF
MO10 003
PO BOX 1000
INDEPENDENCE MO 64051-1000

1 SIERRA BULLETS
P DALY
1400 W HENRY ST
SEDALIA MO 65302-0818

1 ST MARKS POWDER
GENERAL DYNAMICS
R PULVER
7121 COASTAL HWY
CRAWFORDVILLE FL 32327

1 ST MARKS POWDER
GENERAL DYNAMICS
J DRUMMOND
7121 COASTAL HWY
CRAWFORDVILLE FL 32327

NO. OF COPIES ORGANIZATION

1 ST MARKS POWDER
GENERAL DYNAMICS
J HOWARD
7121 COASTAL HWY
CRAWFORDVILLE FL 32327

1 ALLIANT TECHSYSTEMS INC
D A WORRELL
H ZIEGLER
ATK/RADFORD ARMY AMMUNITION PLANT
RADFORD VA 24060

ABERDEEN PROVING GROUND

4 COMMANDER
US ARMY ATC
G NIEWENHOUSE
G POWERS
T HUMISTON
J AYERS
BLDG 400
APG MD 21005

4 COMMANDER
US ARMY TACOM ARDEC
AMSRD AR AEF D
M AMRHEIN
A SOWA
J FONNER
T SAITZ
B305
APG MD 21005

34 DIR USARL
RDRL WM
P PLOSTINS
T ROSENBERGER
M ZOLTOSKI
RDRL WML
J NEWILL
D LYON
RDRL WML A
C MERMAGEN
W OBERLE
J SOUTH
S WANSACK
D WEBB

NO. OF COPIES ORGANIZATION

RDRL WML E
V BHAGWANDIN
I CELMINS
G COOPER
J DESPIRITO
L FAIRFAX
F FRESCONI
J GARNER
B GUIDOS
K HEAVEY
G OBERLIN
J SAHU
S SILTON
P WEINACHT
RDRL WML F
D HEPNER
RDRL WML G
C EICHHORST
W DRYSDALE
M BERMAN
RDRL WML H
C CANDLAND
T EHLERS
L MAGNESS
RDRL WMM F
R CARTER
RDRL WMP
P BAKER
RDRL SLB D
R KINSLER
RDRL HRS B
T FRY